



Chem Soc Rev

Catalytic Reactions within the Cavity of Coordination Cages

Journal:	<i>Chemical Society Reviews</i>
Manuscript ID	CS-SYN-01-2019-000091.R3
Article Type:	Review Article
Date Submitted by the Author:	18-Jun-2019
Complete List of Authors:	Fang, Yu; Texas A&M University System, Chemistry Powell, Joshua; Texas A&M University System, Chemistry Li, Errui; Zhejiang University Perry, Zachary; Texas A and M University System Wang, Qi; Texas A and M University System Kirchon, Angelo; Texas A&M University System Yang, Xinyu; Texas A and M University System, Xiao, Zhifeng; Texas A&M University System zhu, Chengfeng; Hefei University of Technology Zhang, Liangliang; Northwestern Polytechnical University Huang, Feihe; Zhejiang University Zhou, Hong-Cai; Texas A&M University System, Chemistry

SCHOLARONE™
Manuscripts



Chemical Society Review

REVIEW

Catalytic Reactions within the Cavity of Coordination Cages

Yu Fang,^a Joshua A. Powell,^a Errui Li,^b Qi Wang,^a Zachary Perry,^a Angelo Kirchon,^a Xinyu Yang,^a Zhifeng Xiao,^a Chengfeng Zhu,^c Liangliang Zhang,^d Feihe Huang,^b Hong-Cai Zhou^{*a e}

Received 00th January 20xx,
Accepted 00th January 20xx

DOI: 10.1039/x0xx00000x

www.rsc.org/

Natural enzymes catalyze reactions in their substrate-binding cavities, exhibiting high specificity and efficiency. In an effort to mimic the structure and functionality of enzymes, discrete coordination cages were designed and synthesized. These self-assembled systems have a variety of confined cavities, which have been applied to accelerate conventional reactions, perform substrate-specific reactions, and manipulate regio- and enantio-selectivities. Many coordination cages or cage-catalyst composites have achieved unprecedented results, outperforming their counterparts in different catalytic reactions. This tutorial review summarizes recent developments of coordination cages across three key approaches to coordination cage catalysis: (1) cavity promoted reactions, (2) embedding of active sites in the structure of the cage, and (3) encapsulation of catalysts within the cage. Special emphasis on the review involves: (1) introduction of the structure and property of the coordination cage, (2) discussion of the catalytic pathway mediated by the cage, (3) elucidation of the structure-property relationship between the cage and the designated reaction. This work will summarize the recent progress in supramolecular catalysis and attract more researchers to pursue cavity-promoted reactions using discrete coordination cages.

1. Introduction

Natural enzymes are a type of biomacromolecule that play an indispensable role in the biological systems.^[1-3] One of the most important features of the enzyme is the substrate-binding pocket. This pocket serves as a “cave” to encapsulate a substrate and catalyze a given reaction accordingly. Although inorganic, organometallic and artificial catalysts have been investigated for many decades, the gold standard of catalysis, in terms of specificity and efficiency, still belongs to the enzyme. Thus, many attempts have been applied to mimic the structure and functionality of enzymes. Consequently, supramolecular chemists have developed a series of self-assembled artificial systems for this purpose. Pioneered by Lehn, Pedersen, Cram, and Breslow, pure organic supramolecular hosts have evolved well in the past four decades.^[4-8] Crown ether, cryptand, cyclodextrin, calixarene, and cucurbituril were developed and applied for catalyzing

homogeneous reactions in solutions.^[9-12] Those systems are extremely successful and paved ways for their eventual successors. However, because of their limited cavity space, these artificial cavities are often unable to meet the requirements of the development of modern catalytic reactions. Therefore, a new class of supramolecular hosts with tunable cavities is urgently needed.^[13-16]

“Coordination cages”, also known as “Metal-Organic Polyhedrons/Cages (MOPs/MOCs)”, “Metal-Organic Super Container (MOSC)” or “Porous Coordination Cages (PCCs)”, are discrete supramolecular entities composed of metal knots and organic linkers.^[17-22] They not only exhibit aesthetic structural diversity, but also show unique behavior in catalysis. The ability to incorporate functional moieties into the cages make them designable and programmable nanoreactors, often referred to as “Molecular Flasks”.^[23] Furthermore, the intrinsic cavities of coordination cages allow for the encapsulation of catalysts. The cavities surrounding the encapsulated catalysts serve as tunable microenvironment, replicating the guest-binding pocket of the enzyme. Thus, reaction acceleration, substrate selectivity, regio-selection, and stereo manipulation could be expected to be performed within the cavity of coordination cages.^[24,25] In this context, the preparation of supramolecular coordination cages that either promote the reaction themselves or cooperate with catalysts to accelerate or direct chemical transformation is of particular importance and interest. Although discrete coordination cages have been widely explored as supramolecular catalysts,^[26-29] the reaction

^a Department of Chemistry, Texas A&M University, College Station, Texas 77842-3012, USA. E-mail: zhou@chem.tamu.edu; Fax: +1 979 845 1595; Tel: +1 979 845 4034.

^b State Key Laboratory of Chemical Engineering, Center for Chemistry of High-Performance & Novel Materials, Department of Chemistry, Zhejiang University, Hangzhou, 31007, P. R. China.

^c Anhui Province Key Laboratory of Advanced Catalytic Materials and Reaction Engineering, School of Chemistry and Chemical Engineering, Hefei University of Technology, Hefei, 230009, P. R. China

^d Institute of Flexible Electronics (IFE), Northwestern Polytechnical University, Xi'an, 710072, P. R. China

^e Department of Materials Science and Engineering, Texas A&M University, College Station, Texas, 77842, United State

substrates and products are still limited and there are only a handful of systems that can perform asymmetric catalysis.^[30]

Generally speaking, both the cage alone and a cage encapsulated catalyst can be employed for supramolecular catalysis. In the former case, the hydrophobic cavity of the cage may accelerate the reaction by trapping a reaction intermediate or tuning selectivity.^[31-65] Functional moieties could be incorporated into the cavity by the organic ligand to further control the promoted reaction.^[66-78] Among others, reactions such as Diels-Alder cycloadditions, Aza-Cope reactions, Nazarov cyclizations, and hydrolysis reactions have been successfully promoted using functionalized hydrophobic cavities of coordination cages. An alternative approach is to encapsulate an inorganic or organometallic catalyst within the cavity to work synergistically with the cage framework.^[79-88] Furthermore, the cavity can sometimes regulate the orientation or morphology of the encapsulated catalyst, thus further optimizing the reactivity.^[89-91] Based on the ways that coordination cages can function as reaction vessels to perform supramolecular catalysis, three different methods have been developed and are summarized in this context: (1) Cavity-directed catalysis, in which the cage cavity alone serves as catalyst without installation of additional catalytic sites. The cavity provides a hydrophobic environment, substrate proximity, increased local concentration, and substrate pre-organization in order to promote the reactivity and manipulate the selectivity. (2) Incorporation of catalytic sites onto the cage framework for catalysis, in which the catalytic moieties are either derived from organic linkers or introduced as metal centers that are open for substrates access. (3) Encapsulated catalysts for catalysis, in which a variety of catalysts are directly encapsulated by the cage to work synergistically with the confines of the cavity. These cages have been shown to modify the encapsulated catalysts to enhance the reactivity in some cases. Specific examples covering the above three aspects are selected to elucidate the related approach in each section, and the final section briefly presents conclusions and perspectives for future development (Table 1).

2. Criteria for Performing Catalytic Reactions in the Cage

In a supramolecular cage, the cavity is usually surrounded by organic ligands which provide a microenvironment that is distinct from the solution media. Once guest molecules are encapsulated within the confined space, they are isolated from the bulk solvated media. Most of the guest molecules can be regarded as being in their “naked” form when compared to their solvent state because the solvent shells are removed and they cannot freely rotate within the cavity. The specific non-covalent interactions cavity-guest interactions sometimes modulate a chemical transformation either by (1) reducing the free energy or enthalpy of the reaction (i.e. accelerating

substrate binding or converting to product and product releasing), (2) compensating reaction penalty (i.e. trapping an unfavorable reaction intermediate to alter regio- and enantioselectivity), or by (3) significantly increasing local concentration of the reactant, resulting in enhancing the reactivity.

The design criteria for conducting a successful catalytic reaction within the cavity of a coordination cage includes: (1) recognition and encapsulation of the substrate, (2) promotion of the reaction by reducing reaction enthalpy, through trapping an intermediate, or increasing the local concentration of reactants/catalysts, and (3) release of the product to allow catalytic turnover. Additionally, if the catalytic process involves several steps, it is essential that all species formed in the course of the reaction are compatible with the cage. Coordination cages are a suitable system that meets these criteria because the different environments inside and outside of the cavity can discriminate between the substrate and the product. These criteria will become more challenging to meet as more complicated reaction systems are designed. Coordination cages also provide a promising platform for improving compatibility in multistep catalysis due to their modulated structures and functionalities, where multiple catalytic sites could be integrated into one cavity. Use of coordination cages in these systems can also benefit from reactivity enhancements due to the previously mentioned intrinsic merits of the cavity.

To date, hundreds of coordination cage structures have been reported, however, only a select few have been developed for supramolecular catalysis and the catalytic reactions studied are very limited. The main reason for this is the difficulty of engineering the interactions between the cage frameworks and the guest. For most well-studied coordination cages, hydrophobic interactions played a crucial role in substrate binding. However, there are two sides to this coin, as the strong hydrophobic interactions can prevent the cavity from releasing the product. Thus, only stoichiometric reactions, rather than catalytic reactions, have been performed in some coordination cages. Significant effort has been applied to engineer the interactions between the guests and the cage, in order to better balance the desire for encapsulation and release.

Another problem is recyclability. Since coordination cages are soluble in aqueous media or organic solvents, many previously reported coordination cages were employed as homogeneous catalysts, without discussion of recyclability. Solving this recyclability problem is currently a major focus in this field, with several researchers employing their cages as heterogeneous catalysts with excellent reusability.

Finally, coordination cages are not as stable as their solid-phase cousins, Metal-Organic Frameworks (MOFs).^[93] However,

recent advances in zirconium-based cages and multi-nuclear metal cluster-based cages^[94,95] mean this stability problem will not be an issue for the future of coordination cage catalysis.

3. Coordination Cage Promoted Reactions

3.1 Cavity Promoted Reactions

Table 1. Summary of the cages, the catalysts and the reaction types discussed.

Cage	Composite ^a	Charge	Catalyst	Role of Cage	Reaction Type	Ref.
1	M ₆ L ₄	12+	Cavity	Pre-Organization	Diels-Alder	31-36
1	M ₆ L ₄	12+	Cavity	Stabilizing Intermediate	Knoevenagel	44
2	M ₆ L ₄	12+	Cavity	Pre-Organization	Diels-Alder	31
3	M ₄ L ₆	12-	Cavity	Stabilizing Intermediate	Aza-Cope	37-43
3	M ₄ L ₆	12-	Cavity	Stabilizing Intermediate	Nazarov Cyclization	45-49
3	M ₄ L ₆	12-	Cavity	Stabilizing Intermediate	Carbonyl-ene Cyclization	50
3	M ₄ L ₆	12-	Cavity	Stabilizing Intermediate	Prins Cyclization	51
3	M ₄ L ₆	12-	Cavity	Stabilizing Intermediate	Aza-Prins Cyclization	52
3	M ₄ L ₆	12-	Cavity	Stabilizing Intermediate	Hydrolysis	53-58
4	M ₄ L ₆	12-	Cavity	Stabilizing Intermediate	Prins Cyclization	51
5	M ₄ L ₆	8+	Cavity	Stabilizing Intermediate	Hydrolysis	59, 60
6	M ₆ L ₃	12-	Cavity	Stabilizing Intermediate	Hydrolysis	61
7	M ₈ L ₁₂	16+	Cavity	Stabilizing Intermediate	Kemp Elimination	62, 63
8	M ₄ L ₆	8+	Cavity	Stabilizing Intermediate	Cascade	64
9	M ₈ L ₆	16+	Cavity	Stabilizing Intermediate	Cascade	65
10	M ₈ L ₄	0	Brønsted acid	Activate Substrate	Knoevenagel	66, 67
11	M ₃ L ₂	0	Cu (II)	Activate Substrate	A ³ coupling	68
12	M ₄ L ₂	0	[Rh(acac)] ²⁺	Activate Substrate	Hydroformylation	70
13	M ₄ L ₆	2-	[FeFe]-H ₂ ases	Activate Substrate	Water Splitting	71
14	M ₆ L ₈	28+	Ru Complex	Activate Substrate	Photo Hydrogen Evolution	72
15	M ₁₂ L ₆	0	M(salen)	Prevent Aggregation	Epoxidation	73
16	M ₂₄ L ₁₂	0	M(salen)	Prevent Aggregation	Chiral Resolution	74
17	M ₈ L ₆	16+	M-tapp	Activate Substrate	Cyclopropanation	75
18	M ₆ L ₆	8+	COOH	Activate Substrate	Acetal Solvolysis	76
19	M ₄ L ₄	4+	Cu ⁺	Activate Substrate	Redox	77

ARTICLE						Journal Name
20	M ₄ L ₄	4+	Cu ⁺	Activate Substrate	Tetralin oxidation	78
3	M ₄ L ₆	12-	[Cp*(PMe ₃)Ir(Me)] ⁺	Size Selectivity	C-H Activation	79,80
3	M ₄ L ₆	12-	[(PEt ₃) ₂ Rh(COD)] ⁺	Size Selectivity	C-H Activation	81
3	M ₄ L ₆	12-	Et ₃ PAu ⁺	Size Selectivity	Allene hydroalkoxylation	82, 83
4	M ₄ L ₆	12-	Platinum dialkyl complex	Size Selectivity	Alkyl-alkyl elimination	84
21	M ₁₂ L ₂₄	24+	TEMPO, DA	Prevent Deactivation	Tandem	85
21	M ₁₂ L ₂₄	24+	Au complex	Increase Concentration	Hydroalkoxylation	86, 87
21	M ₁₂ L ₂₄	24+	Ru(bda)Het ₂	Increase Concentration	Water Oxidation	88
22	M ₂₄ L ₁₂	0	Pt Nanoparticle	Tune Size	HER	89
23	M ₂₄ L ₁₂	30-, 6-	Ru/Co Nanoparticle	Tune Morphology	Dehydrogenation	90, 91
23	M ₂₄ L ₁₂	30-	[Ru(bpy) ₃] ²⁺ Cl ₂	Tune Reactivity	Photodegradation	92

^a M: metal; L: organic ligand. (The encapsulated metal or incorporated metal or ligands do not count for the composite of the cage)

In this section, we will introduce situations in which the cavity of the supramolecular cage serves as an active site for a variety of reactions. For these cages, neither the metal centers nor the organic ligands alone can catalyze the designated reactions, however, the combination of metals and ligands assembled to form a cavity is capable of catalyzing reactions. We have sorted the reaction mechanisms and roles of the cavity into three major classes: (1) pre-organization of the substrate to accelerate the reaction and yield a regioselective product, (2) stabilization of a reaction intermediate to accelerate the reaction, and (3) capture of an unusual intermediate to alter the reaction route.

3.1.1 Pre-organization of substrates

Rigid self-assembled coordination cages, where the metal knots and organic linkers are connected by robust and reversible bonds, are the earliest supramolecular hosts in which catalysis within the cavity was investigated. For instance, the Fujita research group applied diamine moieties as vertex ligands to enforce a 90° cis capping angle around the square-planar coordination of Pd^{II} and Pt^{II} metals.^[31] Cage **1** has an octahedral geometry and was quantitatively formed in aqueous solutions using a 6:4 metal to ligand ratio. X-ray crystallographic data reveals that cage **1** contains a large, hollow, hydrophobic cavity surrounded by triangular 1,3,5-tris(4-pyridyl)triazine ligands (Figure 1a). It is noteworthy that the cage framework has an overall net charge of 12+, with NO₃⁻ or PF₆⁻ as counter anions. The cavity of cage **1** exhibits excellent organic guest binding capability. By switching to a different triangular 1,3,5-tris(3-pyridyl)triazine ligand, they obtained a bowl shape structure,

cage **2**, which can be regarded as half of cage **1** (Figure 1a). Because of the cationic nature of the structure and the hydrophobic cavity, cages **1** and **2** are both capable of encapsulating neutral aromatic guests and anionic guests. To successfully conduct catalytic reactions within the cavity of cages **1** and **2**, the choice of substrate is critical. In the remainder of this section, we will see that: (1) most of the substrates are aromatic and flat neutral molecules, for which encapsulation by the cage is favorable and (2) it is crucial that the size and shape of the substrates are complementary to the cavity in order to perform the catalytic reaction.

Initially, by using this water-soluble cage **1**, Fujita and co-workers achieved enhanced reactivity towards Diels-Alder reactions of a number of dienes and dienophiles. For example, when 1,4-naphthoquinone and cyclohexadiene were introduced into the cavity of cage **1**, the Diels-Alder reactions were accelerated 113-fold.^[32] The authors proved that both the dienes and dienophiles were encapsulated in a 1:1 ratio in the cavity of the cage. This information indicated that the proximity and pre-organization of the substrates are the primary cause of reaction acceleration.

The same group then attempted a more difficult Diels-Alder reaction between anthracene and *N*-substituted maleimide (Figure 1b).^[33] Without a catalyst, the cycloaddition of these substrates barely proceeds in room temperature, and the dienophile only reacts with the central benzene ring of the diene, giving a 9,10-adduct. However, when the two reactants were encapsulated by coordination cage **1**, the unusual 1,4-adductive products were formed and isolated. As with the

previous substrates, the selective bimolecular recognition and control of the orientation of these two substrates within the cavity of cage **1** dictate the unusual reaction. Furthermore, the reaction yield was increased by cage **1** to >98%, compared to 44% in the absence of the cage. Although it is not a catalytic reaction, cage **1** indeed accelerated the Diels-Alder reaction and, more importantly, altered the regioselectivity. In contrast, cage **2** is capable of catalyzing this transformation (Figure 1c). As little as 10 mol% of cage **2** can efficiently catalyze the reaction and the yield is >99%. The catalysis was furnished by auto-inclusion of the substrates and auto-exclusion of the product by cage **2**.

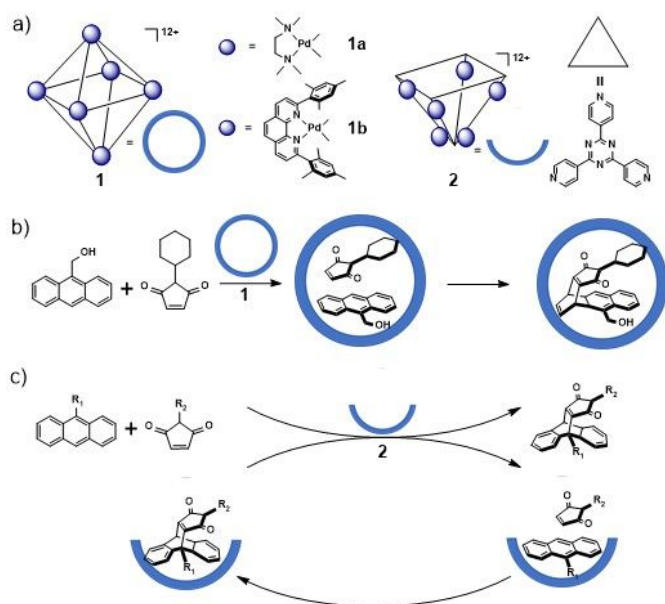


Fig. 1 Fujita Cage for Diels-Alder reactions. a) Structure of octahedral cages **1a** and **1b**, and bowl-shaped cage **2**. b) Diels-Alder reaction accelerated by cage **1a**. c) Diels-Alder reaction catalyzed by cage **2**.

In 2010, Fujita's group reported the Diels-Alder reaction of substituted naphthalene accelerated by cage **1a** (Figure 2a).^[34] Because of the notorious low reactivity for these Diels-Alder reactions, electronic modification of the substrates or harsh conditions usually need to be applied in order to accelerate the reaction. By employing cage **1a**, the Diels-Alder reaction of 2,3-diethylnaphthalene and *N*-cyclohexylmaleimide was dramatically promoted to 64% yield under mild conditions. In contrast, without cage **1a**, the reaction hardly proceeds. The authors found that bulky substrates are required to achieve a satisfactory reaction yield (60-64%). This phenomenon demonstrates that the interactions between the substrates and the cage frameworks are essential (Figure 2b). Because the naphthalene molecule is much smaller than anthracene, it is not sufficiently bulky to form a closely packed ternary complex. For this reason, the naphthalene must be substituted in order to provide sufficient packing and increase the reactivity. In contrast, the Diels-Alder product is bulky enough to facilitate the interactions with the cage by remaining in the cavity of the cage, thus hindering the catalytic cycle. However,

this finding raised a question: is it possible to manipulate the reactivity by varying the relative size of the substrates and the surrounding cavities. This question was answered in 2015 by the same group (Figure 2c). They reported catalytic Diels-Alder reaction of non-substituted naphthalene by an analog of cage **1b** that contained a shrunken cavity. By introducing a bulky ancillary ligand to the vertex of cage **1a**, the cavity volume of the cage was dramatically reduced by 20%.^[35] Cage **1b** with a shrunken cavity showed temporary co-encapsulation of non-substituted naphthalene and *N*-*tert*-butylmaleimide (Figure 2d). As little as 10 mol% of the cage can efficiently catalyze the reaction to give a total isolated 33% yield.^[36] The authors also noted that the cage with the shrunken cavity cannot encapsulate substituted naphthalene, as these substrates are too large to enter the cavity. This prevents the catalytic reaction from occurring and demonstrates that by varying the relative size of the substrate and the cavity, it is possible to manipulate reactivity within the cage.

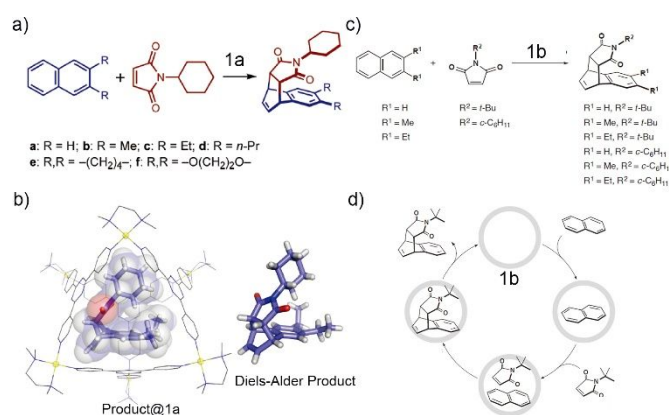


Fig. 2 Fujita Cage for Diels-Alder reactions of naphthalenes. a) b) Diels-Alder reaction of substituted naphthalenes accelerated by cage **1a**. c) d) Diels-Alder reaction of non-substituted naphthalene catalyzed by cage **1b**. Reproduced in part with permission from American Chemical Society from reference 34.

3.1.2 Stabilizing Intermediate

3.1.2.1 Aza-Cope Reaction

Raymond and co-workers have composed a series of supramolecular tetrahedral structures with M_4L_6 stoichiometry ($M = Ga^{3+}, Al^{3+}, Fe^{3+}, Ge^{4+}, Ti^{4+}$, $L = 1,5$ -bis(2',3'-dihydroxybenzamido)naphthalene).^[37,38] In these structures, the four metal atoms are located at the vertices of the tetrahedron and six naphthalene-based bis-bidentate catechol ligands span its edges, forming a T -symmetric, cavity-containing assembly, cage **3** (Figure 3a). The tris-bidentate chelation of the metal centers renders them chiral (Δ or Λ), and the mechanical coupling through the rigid ligands results in the formation of exclusively homochiral assemblies (i.e. $\Delta, \Delta, \Delta, \Delta$ or $\Lambda, \Lambda, \Lambda, \Lambda$). Cage **3** has a 12- overall charge and is water soluble, yet contains a flexible hydrophobic cavity of 350-500 Å³ into which it can bind a broad range of mono-cationic guest molecules. As an anionic cage, cage **3** is prone to capture and stabilize a cationic intermediate with suitable size

and shape to the cavity. This led Raymond and co-workers to focus on a variety of reactions which generate cationic intermediates and to investigate reaction promotion in the presence of cage **3**.

Raymond and co-workers selected the cationic 3-aza-Cope rearrangement as the model reaction to be performed with the cavity of cage **3**. The substrates are ammonium cations (**A**) and should bind to the cavity interior. Sigmatropic rearrangement leads to an iminium cation (**B**), which is subsequently hydrolyzed to the corresponding γ,δ -unsaturated aldehyde (**C**) (Figure 3b). They found that the rearrangement was accelerated when the substrates were encapsulated by the supramolecular cage, especially for the isopropyl-substituted enammonium cation, which experienced an 854-fold rate acceleration.^[39] The authors further revealed that a decrease in the entropy of activation for the encapsulated rearrangement is responsible for the observed rate enhancements, as compared to the free reaction. Furthermore, the spatially restrictive cavity preferentially binds closely packed, preorganized substrate conformations, closely resembling the conformation of the chair-like transition state. In a subsequent study, the same group addressed the question of product hydrolysis through detailed kinetic studies.^[40] They concluded that the iminium product must dissociate from the cavity interior and the assembly exterior before hydroxide-mediated hydrolysis can occur and proposed the intermediacy of a tight ion pair of the polyanionic host with the existing product. The cage can act as a true catalyst since release and hydrolysis facilitate catalytic turnover.

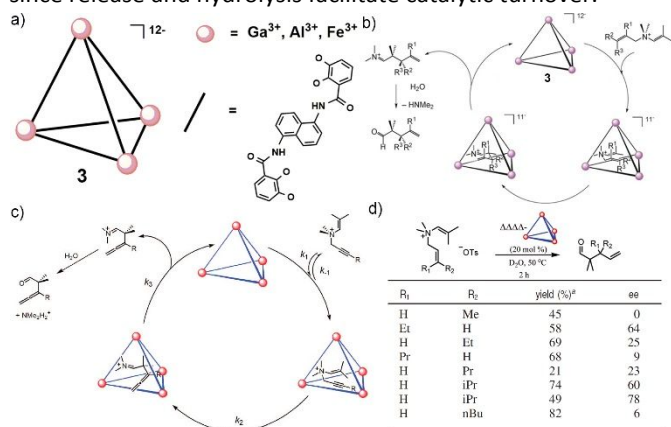


Fig. 3 Raymond Cage for aza-Cope reactions. a) Structure of cage **3**. b) Reaction of the enammonium cation. c) Reaction of propargyl enammonium. d) Chiral Aza-Cope reactions. Reproduced in part with permission from American Chemical Society from reference 37 and 40. Reproduced in part with permission from WILEY-VCH Verlag GmbH & Co. KGaA, Weinheim from reference 38 and 39.

In 2008, the same group tried the more challenging aza-Cope rearrangement of propargyl enammonium cations (Figure 3c).^[41] These compounds react at a much slower rate than the allyl-vinyl substrates, requiring elevated temperatures to obtain useful rates of reaction. In the same manner, substrate encapsulation within the confined host interior

enforces a more reactive conformation that accelerates the rate of rearrangement by factors of up to 184.

Employing supramolecular assemblies in asymmetric catalysis is an important challenge. Raymond and co-workers found that although cage **3** is usually formed as a racemate, addition of (-)-N'-methylnicotinium iodide causes the spontaneous resolution of the two enantiomers (Figure 3d). Furthermore, they applied chiral cage **3** as an enantioselective catalyst for the aza-Cope rearrangement.^[42] High enantioselectivities were achieved (78% ee) for some substrates, but enantioselectivity varied significantly with subtle changes in substrate size and shape. Raymond and coworkers explained that close contact between the substrate and the chiral elements of the host may be responsible for the selectivity of the rearrangement. Nakajima and co-workers provided clearer insights into the mechanism of the rearrangement by using density functional theory (DFT) and *ab initio* molecular orbital calculations.^[43] The authors analyzed the shape complementarity and host-guest interaction in detail and confirmed the origin of the enantioselectivity.

3.1.2.2 Knoevenagel condensation

As a typical dehydration condensation, the Knoevenagel condensation has been of great interest. The reaction is usually catalyzed by weak base, however, by using cage **1**, the Knoevenagel condensation of various aromatic aldehydes can also be promoted under neutral conditions (Figure 4).^[44] The hydrophobic cavity of the cage efficiently binds four molecules of the reaction substrate, 2-naphthaldehyde. When treating this host-guest complex with Meldrum's acid, the condensation products of variously substituted aldehydes were formed in 96% yield with only 1 mol% of cage **1**. In contrast, in the absence of cage **1**, the reaction hardly proceeds under these conditions. Furthermore, they found that the cage **1**-mediated reaction yield was highly dependent on the size of the substrates. The reaction was expected to be initiated by deprotonation of Meldrum's acid to form an enolate. The enolate further attacks the encapsulated aldehyde to generate an oxyanion, which is stabilized by the cationic cage, before dehydration of the oxyanion yields the final product. The as-formed product is spontaneously released from the cavity and replaced with a new molecule of the substrate. This example demonstrates that efficient substrate binding and intermediate stabilization by the cationic cage facilitates the condensation reaction in water media. It provides insight for further developing catalytic reactions by using coordination cage as a synthetic mimic of enzymes.

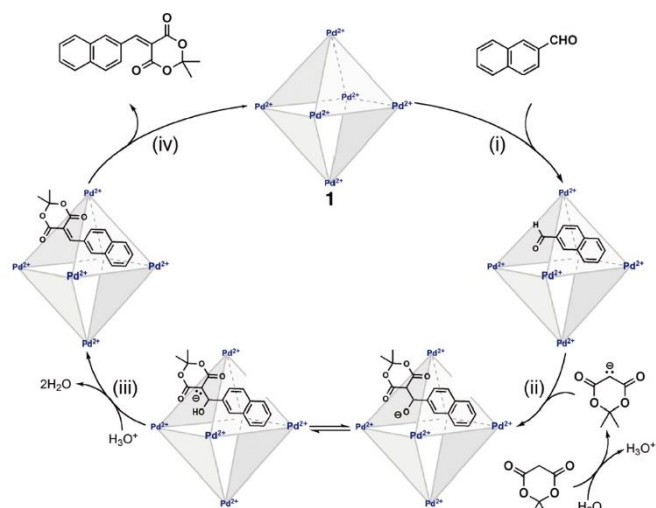


Fig. 4 Knoevenagel condensation catalysed by Fujita cage **1**. Reproduced in part with permission from American Chemical Society from reference 44.

3.1.2.3 Cyclization Reactions

Raymond and co-workers also attempted to exploit the preference of the polyanionic M_4L_6 host **3** for encapsulating mono-cationic guests in accelerating cyclizations. The first example is the Nazarov cyclization, in which a 1,4-dien-3-ol forms a cyclopentadiene. This reaction proceeds via the intermediacy of a diallylic carbocation that undergoes conrotatory electrocyclic ring closure in accordance with the Woodward-Hoffmann rules.^[45] The authors demonstrated that the Nazarov product could be formed in the presence of cage **3** (Figure 5a).^[46] However, the conversion of the initial reaction was low due to inhibition of the reaction rate by the product. To combat this, they developed a way to alleviate product inhibition by chemically converting the product to a poor guest. Specifically, in the **3**-catalyzed Nazarov cyclization, maleimide (**D**) was used as a trapping agent to produce the Diels-Alder adduct of the diene product. The results showed a million-fold rate enhancement of the catalyzed reaction over the uncatalyzed reaction, which achieves a level of rate enhancement comparable to that observed in several enzymes. Raymond and coworkers explained that the million-fold rate increase in the system is due to the combination of an increase in the basicity of the alcohol functionality of the substrate upon encapsulation, pre-organization of the bound substrate, and stabilization of the transition state (**E**) of the electrocyclic reaction. They also found that the reactivities of the three substrates studied are remarkably different when they differ only in stereochemistry at positions remote from the forming carbocation. Furthermore, kinetic analysis and ^{18}O -exchange experiments implied **F** is initially produced as the kinetic product from **G** and **H**, but is immediately converted into the thermodynamic product Cp^*H (Figure 5b).^[47,48] Analysis of the energetics revealed that the regiochemistry of deprotonation in the host-catalyzed reaction is determined by the stereochemistry of an intermediate cyclopentenyl cation **I**, the

structure of which is determined by the alkene stereochemistry of the reactant (Figure 5c).

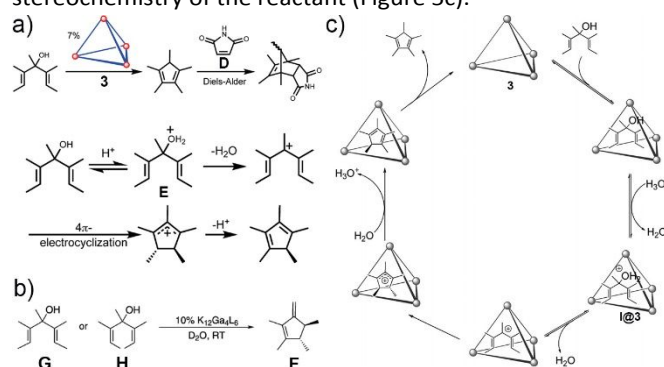


Fig. 5 Nazarov cyclization catalyzed by Raymond cage **3**. a) Nazarov cyclization of 1,4-dien-3-ol catalyzed by cage **3**. b) Kinetic analysis and ^{18}O -exchange experiments. c) Catalytic cycle. Reproduced in part with permission from American Chemical Society from reference 45 and 46. Reproduced in part with permission from WILEY-VCH Verlag GmbH & Co. KGaA, Weinheim from reference 47 and 48.

Recently, Raymond and co-workers also examined the importance of anionic host charge on reactivity (Figure 6).^[49] They demonstrated that although the two isomeric catalysts **3a** and **3b** exhibited similar host-substrate interactions, the difference in overall anionic charge (12^- and 8^-) had a large effect on the reaction rate of Nazarov cyclizations, with an impressive 680-fold difference as a consequence of a 33% reduction in catalyst charge. They experimentally validated the significant stabilizing effect of the anionic host charge in reactions that feature a buildup of cationic charge, determining that the rate increase stems from stabilization of not only the initial protonation step, but also of the subsequent carbocationic intermediates and transition states. This is the first example in which these effects have been experimentally defined in a system involving a synthetic microenvironment.

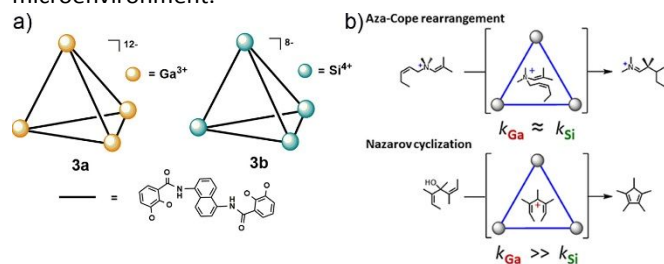


Fig. 6 Nazarov cyclization catalyzed by Raymond cage **3** with different charge. Reproduced in part with permission from American Chemical Society from reference 49.

Raymond and co-workers also used the chiral cage to stereoselectively catalyze carbonyl-ene cyclisation reactions, mimicking the function of enzymes such as terpene synthases.^[50,51] Cage **3** was predicted to be an effective mimic of a terpene synthase, as the cage contained a sterically constricted, hydrophobic interior cavity bounded by cation-stabilizing, π -electron-rich aromatic moieties, which create a similar environment to the active sites of the enzymes. Stoichiometric addition of cage **3** to (\pm)-citronellal resulted in the quantitative conversion of the citronellal to four different

isopulegols. Notably, only trace amounts of the preferred products of acid-catalyzed cyclizations, *p*-menthane-3,8-diols, were observed, indicating that the cage-catalyzed reaction has specificity. Raymond and coworkers explained this preference by suggesting that the constrictive hydrophobic cavity of **3** both protects the cationic cyclized intermediate from water and encourages the cyclisation with the shape of the cage interior. Addition of a slight excess of PETe_4^+ , which binds strongly in the cavity of cage **3**, quenched the reaction, indicating that the cavity of the cage must be available for the reaction to proceed.

To further investigate the conformational selectivity of the encapsulated reaction, citronellal was replaced with gem-dimethyl substituted citronellal or dihydro substituted citronellal.^[50] These compounds were chosen because an increase in the size of substituents typically encourages ring closure. As predicted, in acidic solutions, the gem-dimethyl substituted and the dihydro substituted compounds form different product mixtures. However, when the reaction is mediated by cage **3**, similar distributions of products are obtained. This was surprising, as the cyclizations are mechanistically similar both in acidic solutions and in the cavity of cage **3**. The similarity in observed product distribution for cage **3**-mediated synthesis can be explained by the steric influence of the cage on the guest molecule.

While the early work required post-synthetic separation of the $\Delta\Delta\Delta\Delta$ - and $\Delta\Delta\Delta\Delta$ - enantiomers of cage **3**, Raymond and coworkers later investigated using an enantioenriched ligand containing amide-based chiral directing groups ortho to the catechol to encourage diastereoselective self-assembly (Figure 7a).^[51] Not only did this modified ligand result in the self-assembly of a chiral cage, cage **4**, it also improved the stability of the cage significantly compared to cage **3**. The electron withdrawing behavior of the newly appended amide groups prevents ligand oxidation and decomposition. These groups can also hydrogen bond to the catechol moieties, which further improves stability. Cage **4** could be assembled using either the *R* or *S* isomer of the ligand, with the *R* isomer forming $\Delta\Delta\Delta\Delta$ -**4** and the *S* isomer forming $\Delta\Delta\Delta\Delta$ -**4**. Compared to cage **3**, cage **4** performed carbonyl-ene cyclisation reactions at a rate seven times faster under the same conditions.

Prins cyclisation inside cages **3a** and **4a**, and their pyrene spaced analogs, cage **3c** and **4c**, were compared in a later study by the group. They found that the presence of the chiral directing groups generally did not change the product distributions, however, the preference for *trans* products increases with the larger pyrene spacers (Figure 7b). The more constrictive pockets of cages **3a** and **4a** destabilize the transition state leading to the *trans* product due to steric interactions with the ligands of the cage, while the larger pockets of cages **3c** and **4c** do not have such an effect (Figure

7c). The cage catalysts provided rate accelerations on the order of 10^4 - 10^5 compared to the uncatalyzed reaction.

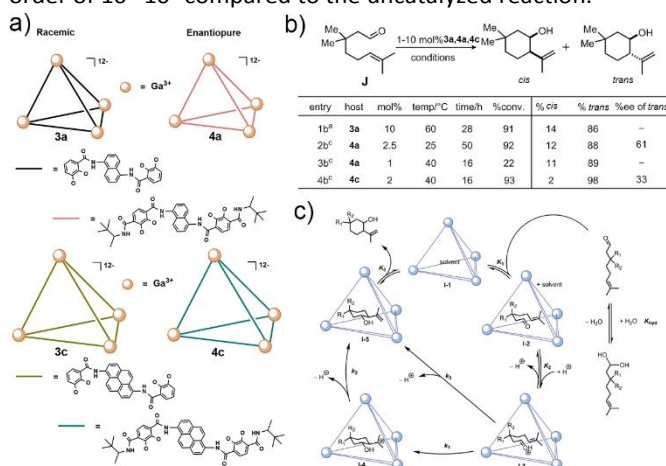


Fig. 7 Prins cyclization catalyzed by Raymond cages **3** and **4**. a) Structure of chiral cages **3** and **4**. b) Reaction selectivity. c) Proposed reaction mechanism.

The same group also performed other cyclizations, such as Aza-Prins cyclizations.^[52] The authors effectively used the steric confinement of the catalyst's interior to make the cyclization reaction efficient and achieve host-mediated enantioselectivity. These reactions represent good examples of extreme divergences in product selectivity observed in catalytic metal-ligand supramolecular enzyme mimics.

3.1.2.4 Hydrolysis

In a behavior analogous to that of enzymes, coordination cages can be used to shift the pKa of guest molecules, thus catalyzing hydrolysis of a variety of guest molecules. The first example is the hydrolysis of orthoformate mediated by a cationic cage **3**. Raymond and coworkers found that cage **3** encapsulates amines and phosphines in their protonated form even at high pH and that the basicity of the protonated amines can increase by up to 4.5 pKa units on encapsulation.^[53,54] The dramatic increase in stability of the protonated species is a consequence of the highly charged cavity favoring encapsulation of the protonated species over the neutral species. The investigation was later expanded to study the mechanism of cage-catalyzed hydrolysis of orthoformates at high pH. These orthoformates are usually highly stable in basic or neutral solutions, however, in the presence of a catalytic amount of cage **3**, triethyl orthoformate was readily hydrolyzed to form a formate ester (and subsequently, formate).^[55] The catalytic reaction is initiated by the neutral substrate entering cage **3** to form a host-guest complex, leading to the resting state of the system (Figure 8). Next, the encapsulated substrate is protonated by water, and undergoes two consecutive hydrolyses within the cavity, releasing two molecules of the alcohol. Finally, the protonated formate ester is expelled from the cage and further hydrolyzed in solution (Figure 8). The overall catalysis obeys Michaelis-Menten kinetics where the initial equilibrium follows a first-order rate-limiting step.

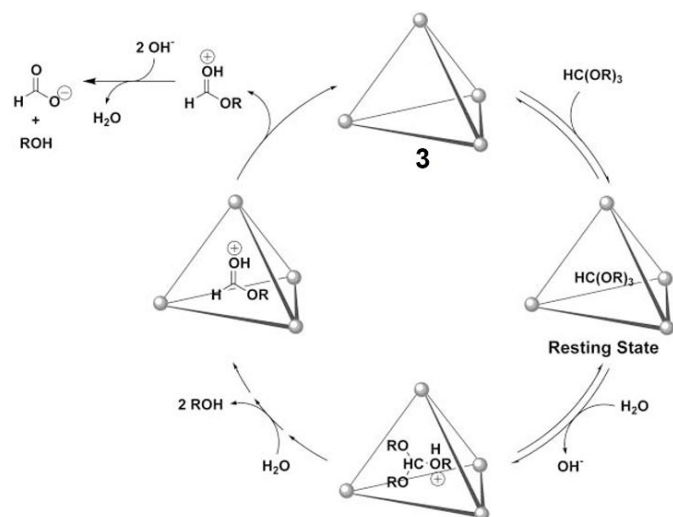


Fig. 8 Hydrolysis catalyzed by Raymond cage **3**. Reproduced in part with permission from American Chemical Society from reference 55.

It is known that the traditional mechanism for orthoformate hydrolysis is A-1, however, the mechanism for the cage-catalyzed one is either a A-2 or A-S_E2 mechanism (Figure 9). The difference between the latter two paths is whether the rate-determining step of the reaction is substrate protonation (A-2) or proton transfer (A-S_E2). The authors investigated solvent isotope effects to differentiate between the two possibilities. It was found that the solvent isotope value is 1.6 when the reaction was performed in the presence of cage **3**, which is consistent with an A-S_E2 mechanism.^[55] This agrees with previous observations that A-S_E2 hydrolysis is more common for orthoformates with stable carbocations.^[56] The rate of the reaction was accelerated by a factor of over 10³ when performed in the cavity of cage **3**.

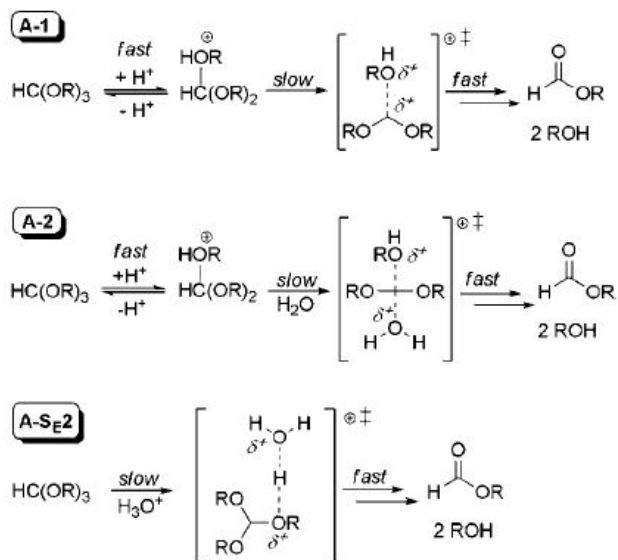


Fig. 9 Three different mechanisms for hydrolysis. Reproduced in part with permission from American Chemical Society from reference 55 and 56.

A similar principle was used to catalytically deprotect acetals under basic conditions.^[57] Small acetals can enter the hydrophobic cavity of cage **3** and become hydrolyzed at high

pH because the cationic protonated intermediates are stabilized by the charge of the cage. Although most of the smallest acetals cannot be observed within cage **3** by NMR, broadening of substrate peaks suggests that the compounds are entering and exiting the cage on a fast timescale. Bulkier substrates enter and exit the cage on a timescale visible to NMR, allowing a 1:1 host: guest complex to be observed. Notably, the largest of the acetals studied, 2,2-dimethoxyundecane and 1,1-dimethoxynonane, were not hydrolyzed to any significant extent, suggesting they are too large to fit inside the cavity of the cage. The hydrolysis product binds less tightly to the cage than the acetal, allowing a relatively high catalytic turnover and preventing catalyst poisoning. As with the cage **3**-encapsulated orthoformate, the encapsulated neutral molecule is the resting state of the catalysis, however, this reaction proceeds via the A-2 pathway, indicating that cage **3** can induce different mechanistic pathways for different substrates. The difference is likely due to the difference in basicity between the two substrates.^[58]

Nitschke and coworkers have demonstrated the utility of coordination cage catalysis for hydrolysis of organophosphate pesticides and chemical weapons. Cage **5**, a tetrahedral Fe₄L₆ cage with a charge of +8, contains a tetrahedral hydrophobic cavity (Figure 10a).^[59] The hydrophobicity of the cavity is a consequence of the glyceryl groups of the ligands pointing outwards and acting as faces of the tetrahedron. The neurotoxic insecticide and chemical weapon simulant dichlorvos can be catalytically hydrolyzed in the cavity of **5** (Figure 10b). Nitschke and coworkers suggest that this is due to the polarization of the O-P bonds by the highly positively charged cage. This allows a nucleophilic attack to occur at the phosphorous atom, resulting in decomposition of the organophosphate.^[60] The hydrolysis products of dichlorvos, dimethyl phosphate and dichlorovinylmethyl phosphate, are not encapsulated by the cage due to their small size and increased water solubility.

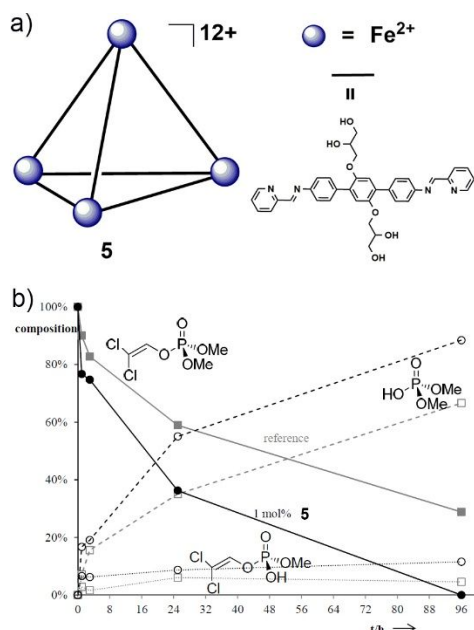


Fig. 10 Hydrolysis catalyzed by Nitschke cage 5. Reproduced in part with permission from WILEY-VCH Verlag GmbH & Co. KGaA, Weinheim from reference 59 and 60.

Mukherjee and co-workers prepared a palladium-based trigonal prism and applied it for a cascade dehydration reaction.^[61] The cage consists of six palladium metal atoms and three tetraphenylethylene (TPE) ligands, to form a prism shape cage 6 (Figure 11a). The cage is cationic and has a hydrodynamic radius of about 12.81 Å according to diffusion-ordered NMR spectroscopy. They found that the cage can efficiently catalyze the one-pot pseudo-three-component synthesis of tetraketones (**K**) and the corresponding xanthenes (**L**) in water. They can selectively obtain tetraketones and the intermediate xanthenes in the same yield (91%). They also performed the reaction with a broad range of substrates, and achieved reaction yields in the range of 85-99%. The hydrophobic cavity of the cage serves as a molecular vessel to perform dehydration reactions (Figure 11b). Moreover, the nano-confinement effect promotes the otherwise unfavorable dehydration reactions in water. Initially, the enolate form of 5,5-dimethylcyclohexane-1,3-dione (**M**) reacts with the encapsulated substrate, an aromatic aldehyde, to generate oxyanion intermediate followed by rapid loss of water to generate Knoevenagel product (**N**). Another molecule of **M** reacts with **N** to generate another oxyanion intermediate. This intermediate is protonated by water to afford the non-cyclized product **L**. Because product **L** is too large for the cavity of the cage, it will be released from the cage and precipitate from the solution. Thus, intermediate **L** can be isolated in the presence of the cage. However, by elevating the reaction temperature, the encapsulated **L** will proceed intramolecular cyclization and generate the final product, **K**. This approach provides a platform for selective isolation of both cyclized xanthenes and their corresponding non-cyclized intermediates by simply changing the reaction temperature.

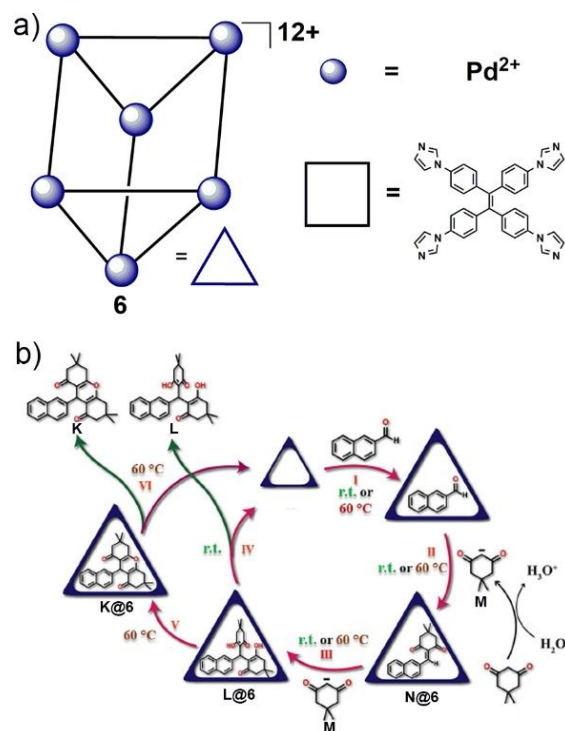


Fig. 11 Hydrolysis catalyzed by Mukherjee cage 6. Reproduced in part with permission from WILEY-VCH Verlag GmbH & Co. KGaA, Weinheim from reference 61.

3.1.2.5 Kemp elimination

In 2016, Ward's and Williams's groups reported a cube-shape coordination cage, cage 7, and applied it as a catalyst in a Kemp elimination reaction.^[62,63] The backbone of the cage is assembled from eight cobalt ions and twelve linear chelating organic linkers (Figure 12a). The cage is water-soluble, and the hydrophobic interior cavity is ~400 Å³ in volume. Importantly, they found that only neutral guests bind strongly while the cage shows a weak affinity for anionic compounds, which indicates guest encapsulation and release can be controlled by pH.

The Kemp elimination performed in cage 7 involves the reaction of benzisoxazole with hydroxide to yield 2-cyano-phenolate, by using this unique cage (Figure 12b).^[62] Because the benzisoxazole substrate is neutral, cage 7 binds it very strongly, with an association constant of $K_{\text{ass}} = 4 \times 10^3 \text{ M}^{-1}$. On the other hand, the ion-pairing effect facilitates the accumulation of hydroxide ions on the surface of the cage. The increased local concentration of hydroxide ions accelerated the maximum observed rate by a factor of 2×10^5 compared to the uncatalyzed reaction. The reaction promotion here is caused by the encapsulated benzisoxazole being in close proximity to the surface hydroxide ions of cage 7. Competing anions, such as Cl⁻, can replace the hydroxide on the cage surface, thus suppressing the catalysis.

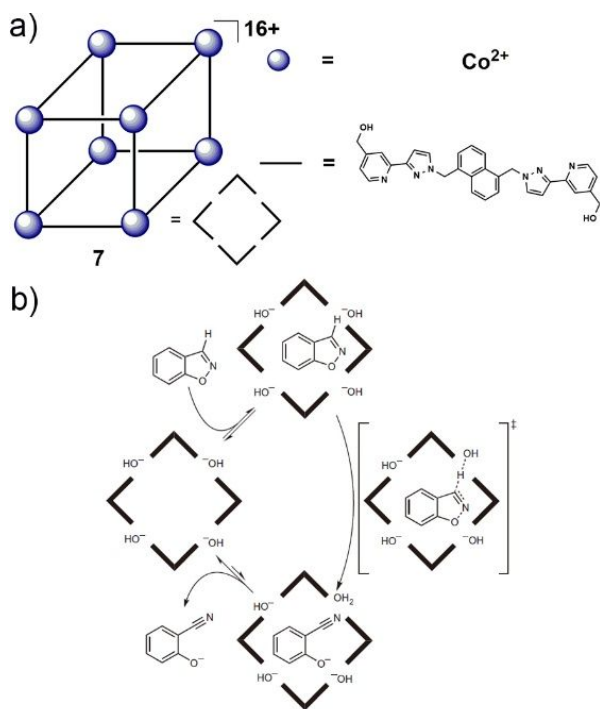


Fig. 12 Kemp elimination catalyzed by Ward cage 7. Reproduced in part with permission from Springer Nature from reference 62.

In 2018, the same group investigated anion inhibition and autocatalysis for the Kemp Elimination by using the same cage. In contrast to other cages, the counter anions of cage **7** are located exclusively at the surface of the cage, while the cavity is filled by water molecules. The original cationic cage **7** has a BF_4^- counteranion, however an analogue with a Cl^- counteranion can be prepared using Dowex resin. In this analogue, Cl^- ions, which are more easily desolvated than OH^- ions, replace the OH^- ions on the cage surface, thereby separating the hydroxide ions and the encapsulated substrate. Therefore, the reaction rate of the catalysis gradually decreases with increasing the concentration of Cl^- ions. Interestingly, when the reaction is more inhibited, the product (2-cyanophenolate) starts to act as a base and displace halide ions on the cage surface. Since the product-halide ion exchange is fast, the autocatalysis is not obvious. The autocatalytic route dominates only when the reaction is quenched by accumulation of the chloride around the cage. The insights obtained from this research paved the way for the use of coordination cages for general catalysis.

3.1.2.6 Cascade reactions

Since the cavity of the coordination cage provides a specific microenvironment which is distinct from the bulk solvent, it is possible to perform cascade reactions in the presence of the cage. One of the advantages of using coordination cage for the cascade reaction is that it can considerably reduce the undesired reaction pathways, thus yielding a single product. Another merit is that the microenvironment of the

coordination cage can stabilize the uncommon intermediates, which facilitates cascade reaction.

In 2013, Nitschke's group reported a self-organizing chemical "assembly line" consisting of a mixture of multiple chemical precursors which is capable of transforming a furan substrate to a low-energy intermediate (**O**), then exclusively to the product (5-hydroxy-3-(nitromethyl)dihydrofuran-2(3H)-one).^[64] What is remarkable of the "assembly line" is the *in situ* self-assembly of the rationally designed metal-organic cage, cage **8**, and the fact that there is no interference between the two catalytic cycles and the formation of the cage (Figure 13a). The first catalytic cycle involves the hetero-Diels-Alder cycloaddition of furan with singlet oxygen ($^1\text{O}_2$) generated by the catalytic activity of the methylene blue. The product of the first cycle, a high-energy endoperoxide intermediate, is encapsulated by the cage and transformed to a lower-energy fumaraldehydic acid intermediate **O**. In this process, the self-assembled cage selectively functionalizes the endoperoxide in the presence of other chemicals in the system under mild conditions. Finally, 1,4-addition of nitromethane to intermediate **O** catalyzed by L-proline-gives the final product (Figure 13b). With a series of control experiments, the authors were able to identify the essential role of the cage in the transformation from endoperoxide to **O** and eliminate the possibility of other competitive pathways. Additionally, the outcome of this "assembly line" is highly dependent on the "input", meaning the removal of any component in the system would change the final product. In addition, this "assembly line" can be easily scaled up 50-fold. Unlike the traditional synthesis, the final product does not require column chromatography to be isolated.

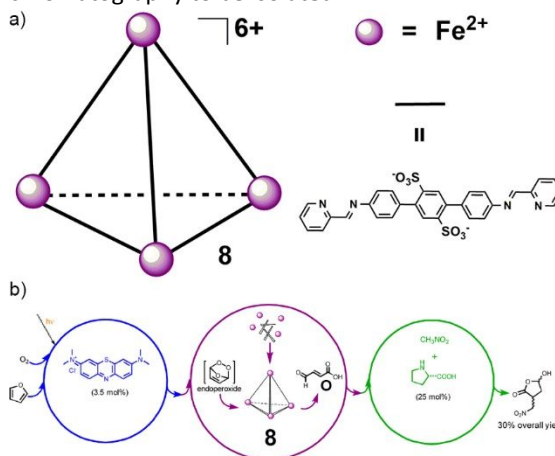


Fig. 13 Cascade reaction catalyzed by Nitschke cage **8**. Reproduced in part with permission from American Chemical Society from reference 64.

Cui's group reported two hexahedral cages that contain no active sites but can still greatly promote chemical transformations, owing to the weak $\text{CH} \cdots \pi$ interactions between the cages and the substrates.^[65] Two tetraphenylethylene (TPE) based cages with Zn^{2+} metal knots, **9a** and **9b**, feature hydrophobicity, flexible cavities, tunable

size, and rich π -electron density that may accommodate aromatic substrates (Figure 14a). Cages **9a** and **9b** manipulate the uptake and release of a variety of guests and accelerate the cascade condensation and cyclization of anthranilamide and aromatic aldehydes to nonplanar 2,3-dihydroquinazolinones (Figure 14b). Initially, the reactant anthranilamide was encapsulated by the hydrophobic cavities of cages **9a** and **9b**. When an aromatic aldehyde is co-encapsulated within the cavity of the cage, an intermolecular condensation takes place to form a cage-encapsulated intermediate. Finally, the amide nitrogen on the activated imine group undergoes intramolecular nucleophilic attack followed by a 1,5-proton transfer to give the final product, a nonplanar 2,3-dihydroquinazolinone. Because the product has an unfavorable nonplanar configuration, it is easily expelled from the cage once formed (Figure 14c). Here, the cage serves as a host to co-encapsulate the two reactants, and stabilize the uncommon intermediate, thus promoting the cascade reaction. The association constants (K_a), determined by UV-Vis titration experiments, suggest that the cages catalyze the reaction as turnover processes, based on the uptake of the substrate and release of the product. The rate is enhanced by factors of up to 38,000 and the rate did not decrease over time. Control experiments determined that free Zn ions had no catalytic effect, proving that catalysis exclusively occurs within the cage cavities. Additionally, the cage with the larger pore, **9b**, shows higher catalytic performance than **9a** under identical conditions, as the large pore facilitates easier mass transport.

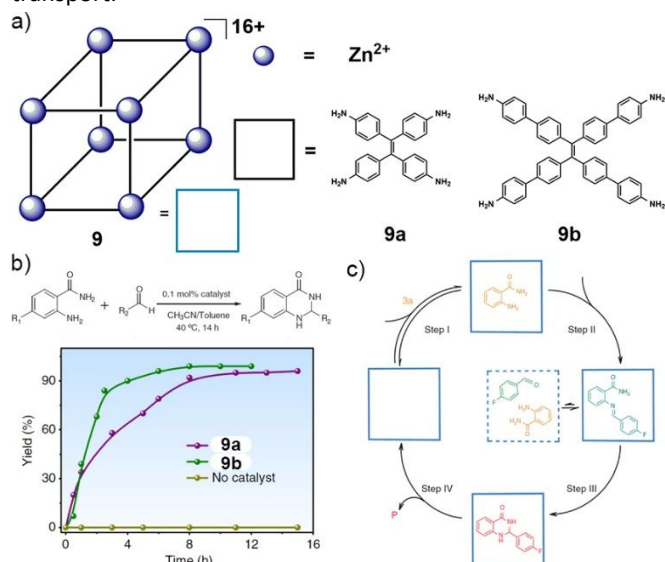


Fig. 14 Cascade reaction catalyzed by Cui cage 9.

3.2 Embedded Active Sites within the Cage

The second approach to coordination cage catalysis is to incorporate active sites into the structure of the cage. Here, the cavity itself is no longer considered an active site, however, it still plays a significant role during the catalytic cycles. Some active sites are generated through cage formation. These active sites are expected to directly activate

the substrate to facilitate the reaction. Other active sites are incorporated onto ligands either pre-synthetically or post-synthetically to form a reactive cage. Since catalytic reactions are taking place around the active sites, the cage itself can perform tasks such as: (1) activating the substrate, (2) isolating catalysts to prevent aggregation, and (3) increasing local catalyst concentration to increase reactivity.

Another example of a Knoevenagel condensation promoted by a coordination cage was reported by Wang et al.^[66,67] The cylindrically-shaped cage **10** is constructed from divalent transition metal ions ($M = \text{Co}^{2+}$ or Ni^{2+}), 4,4'-methylenedibenzoic acid, and sulfonylcalix[4]arenes.^[66] There are two sulfonylcalix[4]arenes located at the vertices of the cylinder, while tetra-nuclear metal clusters connect the capping ligand with four dicarboxylate linkers on the edges (Figure 15a). When the 4,4'-methylenedibenzoic acid is replaced with a methyleneamino moiety, an analog cage **10b** with Lewis-basic active sites was obtained. Wang's group found that **10a** and **10b** are efficient catalysts for the nucleophilic addition of malononitrile to 2-naphthaldehyde, giving a 92% yield. In addition, shape selectivity of the substrate was only observed in **10a**, and not in **10b**.^[67] They found that the Knoevenagel condensation proceeds when the aldehyde substrate has a similar diameter and shape to the cavity of cage **10a**. The metal-bound water molecules in the cavity of cage **10a** serve as Brønsted acids and catalyze the condensation of various aromatic aldehydes in moderate yields (33-62%). These examples exhibit selective substrate recognition and electrostatic/allosteric regulation that result in switchable supramolecular catalysis (Figure 15b). These purpose-specific substrate dictators can be engineered using coordination cages to modulate chemical process in asymmetric catalysis, photocatalysis, and other related areas.

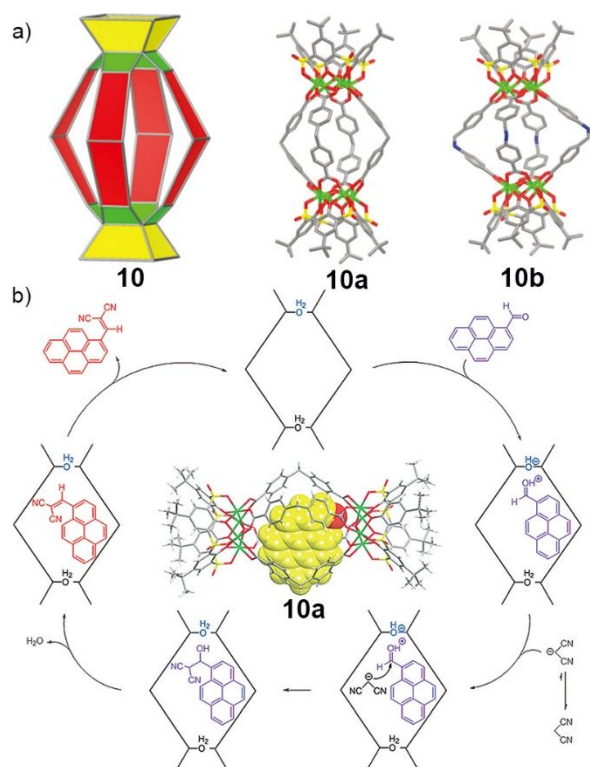
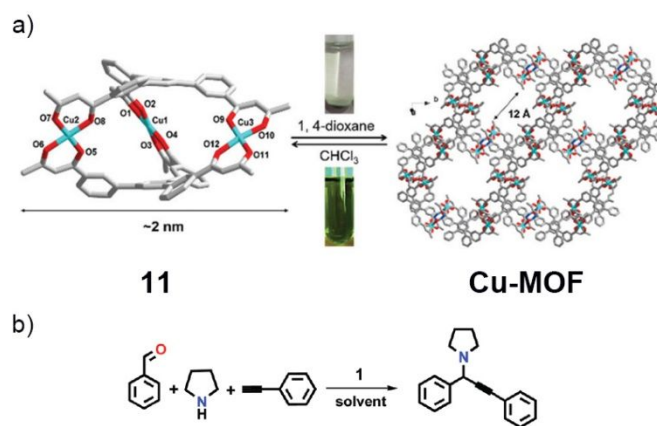


Fig. 15 Knoevenagel reaction catalyzed by Wang cage **10**. Reproduced in part with permission from WILEY-VCH Verlag GmbH & Co. KGaA, Weinheim from reference 67.

Dong and co-workers reported a discrete metal–organic cage, cage **11**, by the assembly of $\text{Cu}(\text{OAc})_2$ and a new tripodal β -diketonate ligand.^[68] The Cu(II) center lies in a quasi-square planar $\{\text{CuO}_4\}$ coordinated environment and two twist tripodal ligands link three Cu(II) ions into an elliptical molecular cage. Since cage **11** contains coordinatively unsaturated Cu(II) centers, it can be used as a homogeneous catalyst to highly promote A^3 coupling reactions in a polar organic medium (Figure 16). By optimizing the reaction conditions, the authors studied the scope of this A^3 coupling with various substrates. Using either aldehydes with various functional groups, such as $-\text{CH}_3$, $-\text{NO}_2$, $-\text{OCH}_3$, $-\text{F}$, $-\text{Cl}$ and $-\text{Br}$, or substituted aromatic alkynes, the reactions proceeded smoothly in high yield. Furthermore, cage **11** could be readily separated from the reaction system via reversible formation of the insoluble Cu(II)-MOF, which forms upon addition of 1,4-dioxane and exhibits good cycling performance.



Entry	T ($^{\circ}\text{C}$)	Solvent	11 (mol%)	t (h)	Yield ^b (%)
1	25	CHCl_3	3	24	98
2	25	CHCl_3	1	24	94
3	25	CHCl_3	0.3	24	84
4	25	THF	3	24	95
5	25	Toluene	3	24	89
6	25	CH_3OH	3	24	57
7	25	CH_3CN	3	24	82
8	40	CHCl_3	3	2	5.3
9	50	CHCl_3	3	2	81
10	60	CHCl_3	3	2	98
11	25	CHCl_3	—	2	9
12	60	CHCl_3	—	2	13

Fig. 16 A^3 coupling catalyzed by Dong cage **11**.

Zhou and co-workers developed a dicopper paddlewheel-based coordination cage and investigated cyclopropanation catalysis.^[69] They first prepared a linear alkyl functionalized coordination cage through condensation reactions, in order to enhance the solubility of the cage, before applying the cage as a homogeneous catalyst for cyclopropanation reactions of styrene with EDA. It was found that 1 mol% of the cage can promote the reaction to give 89% of yield and 2.7:1 ratio of trans/cis selectivity. In control experiments, no acceleration was observed when applying a similar cage without surface functional groups. These results suggest that functionalization can be an efficient way of generating active sites and engineering the reactivity of supramolecular catalyst.

The Reek group developed a novel box-shaped coordination cage, cage **12**, based on bis- $[\text{Zn}^{\text{II}}(\text{salphen})]$ and 3-pyridyl-substituted monodentate phosphoramidite ligands (Figure 17).^[70] Since there are phosphorus atoms pointing toward the cavity to act as a binding site, a $\text{Rh}(\text{acac})(\text{CO})_2$ complex can be readily installed in the cavity to form a reactive species, $[\text{Rh}(\text{acac})]^{2+}$. By taking advantage of this catalyst-cage composite, Rh-catalyzed asymmetric hydroformylation of cis- and trans-2-octene can be performed with an excellent conversion ratio and selectivity. In the absence of the cage, the 2-methyl aldehyde was preferentially obtained over the 2-ethyl aldehyde (methyl:ethyl = 61:39) and the enantiomeric ratio is relatively low (26%). In contrast, when applying **Rh@12** as the catalyst, the regioselectivity was reversed and the b-type aldehyde product is the major product (methyl:ethyl =

40:60). More importantly, the enantiomeric ratio is dramatically increased to 52%. By elevating the temperature, the conversion can be further increased to 36% and 79% for *trans*-2-octene and *cis*-2-octene, in the presence of **Rh@12**. A range of olefin substrates were studied, and it was found that the highest conversion ratio was achieved for styrene (80%) and the highest enantioselectivity was achieved for *cis*-2-octene (93:7). This research demonstrated asymmetric hydroformylation of internal alkenes via a chiral catalyst encapsulated within a confined cavity of a coordination cage approach. The chiral microenvironment generated by the coordination cage afforded extraordinary conversion and enantioselectivity for a variety of olefin substrates.

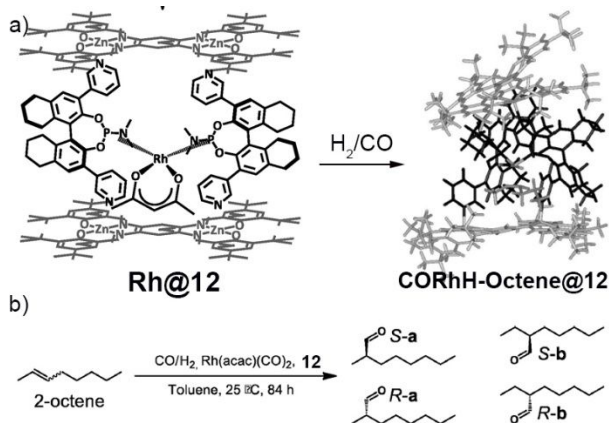


Fig. 17 Asymmetric hydroformylation catalyzed by Reek cage 12. Reproduced in part with permission from American Chemical Society from reference 70.

In 2013, the Duan group reported a basket-like tetragonal coordination cage **13** made of cesium metal ions and bis-bidentate ligand with an N-O pocket (Figure 18).^[71] They found that a biomimetic [FeFe]-H₂ase model catalyst can be readily encapsulated by the cage. Both the photoactive cage and the encapsulated catalyst are essential for the light-driven H₂ production when employing NⁱPr₂EtH-OAc as the sacrificial electron donors. The cage works as the photosensitizer and transfers the electron to the catalyst, owing to the efficient π-π stacking of adenosine aromatic rings and the benzene rings of the ligand. They found that the turnover number (TON) of H₂ evolution was up to 30 with an initial turnover frequency (TOF) of about 11 h⁻¹. This system exhibits enzymatic dynamic behavior, which may be applicable for solar-driven splitting of water.

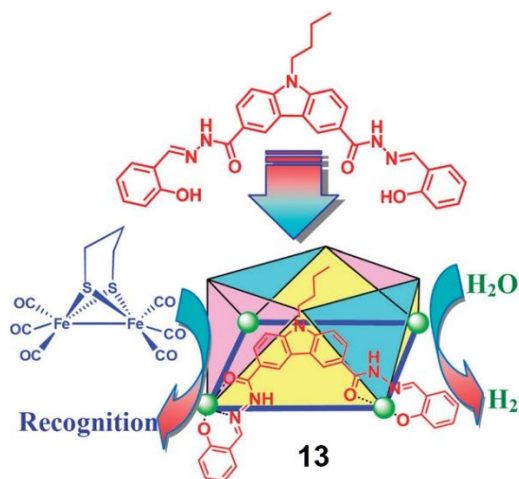


Fig. 18 Water splitting catalyzed by Duan cage 13.

The Su group developed a homochiral heterometallic coordination cage, cage **14**, and investigated the regio- and stereoselectivity of the product formed in the catalyst-containing cage (Figure 19).^[72] The cage adopts an octahedral geometry with palladium metal ions located at the vertexes and the photo-hydrogen-evolving ruthenium complex placed at the faces, to give an M₆L₈ stoichiometry. They found that the cage encapsulates naphthol guests, and performs an unusual regioselective 1,4-coupling to yield 4-(2-hydroxy-1-naphthyl)-1,2-naphthoquinones in excellent yield (up to 96%) and a reasonable enantiomeric excess ratio (up to 58%). The active site is the embedded ruthenium complex, which is a typical photo-driven hydrogen evolving catalyst. Upon irradiation at 453 nm, electron transfer from a photoactive Ru center to a Pd ion gives an intramolecular charge separation and excited state of cage **14**. The excited cage then oxidizes the naphthol through single-electron transfer to give a radical species. By inter- and intra-molecular radical transfer, the 1,4-coupled dimer product was exclusively formed. Furthermore, the chiral environment influences the enantioselectivity. This unusual dimerization constitutes a rare example of asymmetric induction in biaryl coupling by making use of coordination cages with the dual functionalities of photoredox reactivity and stereoselectivity.

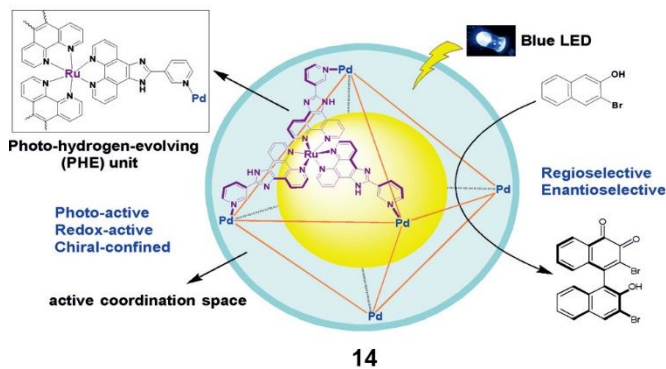


Fig. 19 Selective 1,4-coupling catalyzed by Su cage 14. Reproduced in part with permission from WILEY-VCH Verlag GmbH & Co. KGaA, Weinheim from reference 72.

In 2018, Cui's group designed and synthesized a series of tetrahedral coordination cages (**15-M**) with Cp_3Zr_3 (Cp = cyclopentadienyl) clusters and bidentate chiral $\text{M}(\text{salen})$ ($\text{M}=\text{Mn}$, Fe , and Cr) linkers (Figure 20a).^[73] They can obtain not only homoleptic cages with the same $\text{M}(\text{salen})$ moiety, but also heteroleptic cages with different $\text{M}(\text{salen})$ moieties. These cages are also intrinsically chiral and can have different combinations of configurations – either a homoconfiguration or a blend of heteroconfigurations (Figure 20b). By employing these cages as homogeneous catalysts, they found that **15-Mn** catalyzed the epoxidation of 2,2-dimethyl-2H-chromene to give 65–89% conversions and 83–94% ee of the epoxide (Figure 19c). In contrast, the free $\text{Mn}(\text{salen})\text{Cl}$ catalyst can only achieve 47–84% conversions and 83–91% ee. The chromium version of the cage is capable of promoting the reaction of 2,2-dimethyl benzopyran oxide with aniline, affording 96% conversions with 20% ee of the product. More interestingly, both the heteroleptic cage **15-MnCr** and a 1:1 mixture of homoleptic cages **15-Mn** and **15-Cr** can catalyze a sequential reaction. Compared to the cage mixture, heteroleptic **15-MnCr** shows improved TOF (99 h^{-1} vs 84 h^{-1}), although the number of active sites is identical. This phenomenon indicates that additional cooperative effects are at play in **15-MnCr** to improve the catalytic performances compared to a simple mixture of the two active sites. Since the cage is chiral, **15-MnCr** can also catalyze the sequential epoxidation/ring-opening reactions of 2,2-dimethyl-2H-chromene and its derivatives with anilines, affording high ee values (91–99.9%). These single- and mixed-linker coordination cages not only stabilize chiral salen catalytic centers but also concentrate reactants, leading to much-improved reactivity and stereoselectivity. This research establishes mixed-linker coordination cages as a successful platform for engineering supramolecular catalysis by tuning multiple active sites.

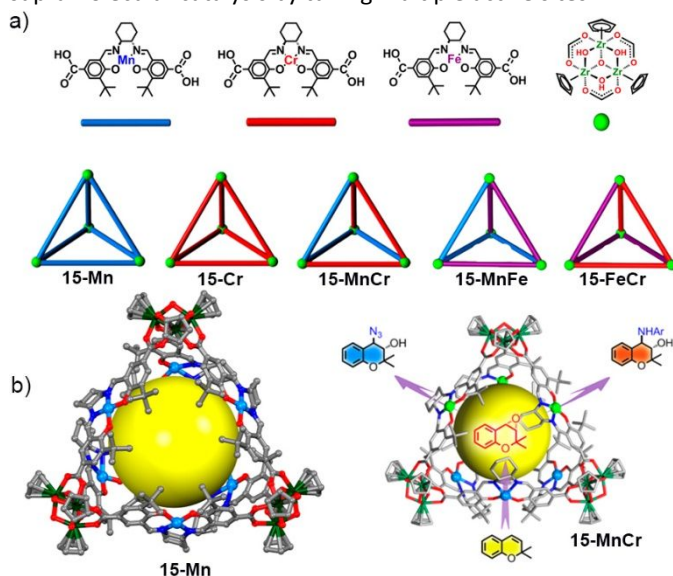


Fig. 20 Sequential epoxidation/ring-opening reactions catalyzed by Cui cage 15. Reproduced in part with permission from American Chemical Society from reference 73.

Cui's group developed another $\text{M}(\text{salen})$ -incorporated chiral coordination cage, cage **16**, with octahedral geometry.^[74] The cage consists of six Zn_4 -*p-tert*-butylsulfonylcalix[4]arene clusters as vertices and eight $\text{Mn}(\text{salen})$ -derived dicarboxylic acids as linear linkers. The cage is equipped with a large hydrophobic cavity (3944 \AA^3) surrounded by chiral active sites, making it a potential supramolecular catalyst. They found that as little as 1.0 mol% of cage **16** sufficiently performs resolution of secondary alcohols, affording 52–62% conversion with 81–99.1% ee of the products (Figure 21). The kinetic study suggests that cage **16** outperforms free $\text{Mn}(\text{salen})$ in terms of conversions and %ee values. Fixing the salen catalyst in the cage framework efficiently prevents catalyst dimerization and increases substrate-catalyst proximity. This work provides an effective method to achieve high catalytic reactivity and enantioselectivity by using judiciously designed supramolecular catalysts. The development of this field will promote the design of discrete functional coordination cages from chiral ligands/catalysts for enantioselective processes.

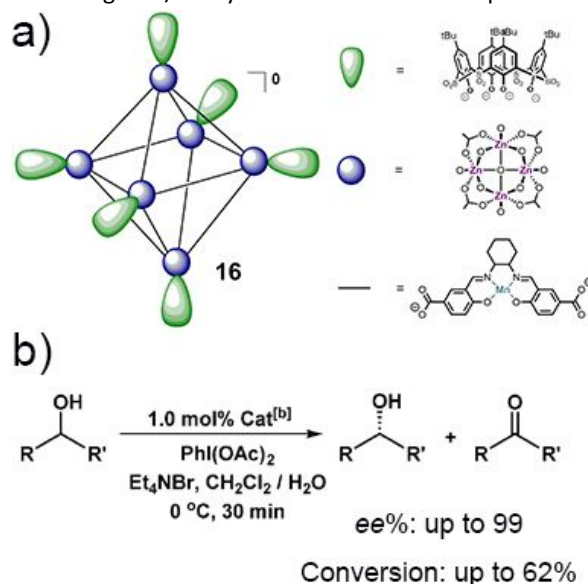


Fig. 21 Chiral resolution catalyzed by Cui cage 16. Reproduced in part with permission from WILEY-VCH Verlag GmbH & Co. KGaA, Weinheim from reference 74.

Metalloporphyrins are widely recognized as multi-functional catalysts, however, they have rarely been introduced into supramolecular cages. In 2013, Reek and co-workers reported a cubic cage, cage **17**, that efficiently encapsulates tetra(4-pyridyl)metalloporphyrins in its cavity and applied it in radical-type reactions (Figure 22).^[75] The cage itself is composed of Zn-substituted tetrakis(4-aminophenyl)porphyrin (Zn-tapp), 2-formylpyridine, and iron(II) trifluoromethane-sulfonate. When treating cage **17** with Zn-tapp or Co-tapp , 1.0 eq. of the guest can be encapsulated within the cavity of cage **17** to form **Co-tapp@17**. To investigate the “caging effect” on the encapsulated Co-tapp , they conducted transformations of diazo compounds. The yield of radical cyclopropanation of styrene with ethyl diazoacetate catalyzed by **Co-tapp@17** is

50%, and the turnover number is 60. When free Co-tapp catalyst was applied, only 7% yield and a TON of 9 were obtained. The superior activity of **Co-tapp@17** compared to non-encapsulated analogs in radical-type transformations is because the shielded environment of the cavity limits the undesirable side reactions of the radical intermediates. This result demonstrates that the activity of a transition metal catalyst can be dramatically enhanced by encapsulation within a supramolecular cage.

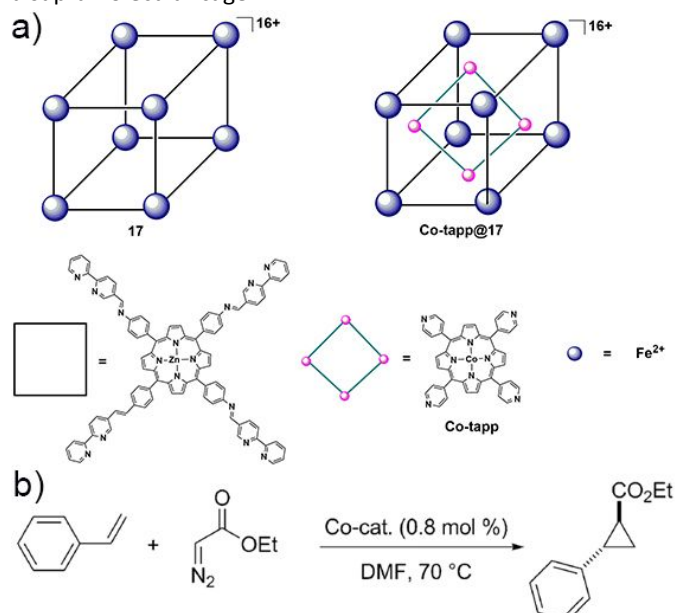


Fig. 22 Styrene cyclopropanation catalyzed by Reek cage **Co-tapp@17**. Reproduced in part with permission from WILEY-VCH Verlag GmbH & Co. KGaA, Weinheim from reference 75.

Hooley's group introduced a rationally designed iminopyridine cage catalyst, cage **18**, with endohedral acid groups that can provide up to 1000-fold rate enhancement and improved selectivity of acetal solvolysis (Figure 23).^[76] After considering the advantages and disadvantages of linear ligands, bent ligands, octahedral metals, and various coordination angles, the authors decided to use an extended 2,7-dianilino-fluorene scaffold for the creation of a functionalized cage. Cages **18a** and **18b** were prepared with an unfunctionalized ligand and acid-functionalized ligand respectively. It was found that the rate of the acetal solvolysis dramatically increased when performed in cage **18b** due to the cage structure showing an affinity to the acetals, as confirmed by NMR and Stern-Volmer analysis. Molecular modeling of cage **18b** isomers suggests that the acid groups are mostly positioned toward the internal cavity. Although cage **18a** also has the affinity to the acetals, it does not possess acid functional groups for catalysis. Compared to cage **18b** (99% conversion), the unfunctionalized cage **18a** and the control ligand **P**, which has acid groups but will not form a cage, shows very low conversion percentage (1% and 7%, respectively). It is worth noting that compartmentalization is another advantage of the cage catalyst. As shown in the cascade reaction, a tandem cage-to-cage interconversion occurs. The combination

of the improved reactivity and the compartmentalization of the acid groups in cage **18b** enables it to be an excellent cascade catalyst.

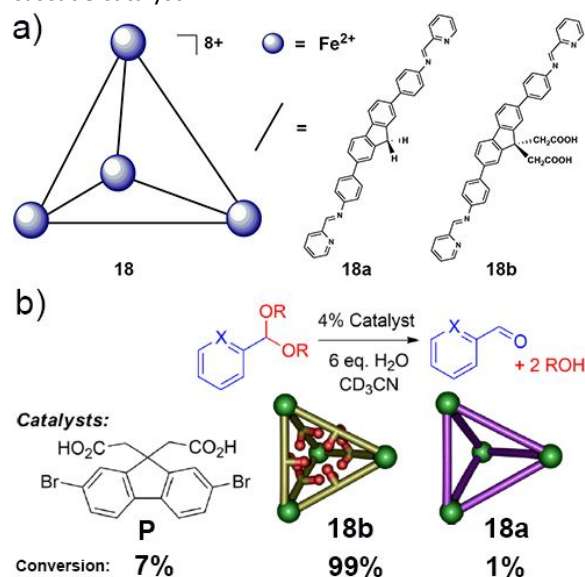


Fig. 23 Acetal solvolysis catalyzed by Hooley cage **18**. Reproduced in part with permission from American Chemical Society from reference 76.

Su and co-workers reported a series of Cu⁺ cuboctahedral coordination cages, cages **19** and **20**, by using a bulky triangular ligand and different Cu⁺ salts (Figure 24).^[77] These cages show redox stability, relying on counteranions, and reactivity towards arene C–H bond activation. In cage **19**, each Cu⁺ ion adopts trigonal coordination geometry to link three (1,3,5-tris(1-benzylbenzimidazol-2-yl)benzene) ligands and each ligand takes on a propeller conformation in which the three benzimidazole rings are twisted relative to the central benzene ring to connect three Cu⁺ ions. Through anion exchange, the redox-inert cage **19** can be converted to the redox-active cage **20**. When the redox-active cages **20a** and **20b** are left in the mother liquid for several days, hydroxylation of the ligand under ambient conditions was observed to transform cages **20a** and **20b** to the Cu²⁺ complexes **20c** and **20d** respectively. In contrast, cages **19a** and **19b** are relatively stable, remaining unchanged even when kept in solution for several months. The authors explained that, since the guest encapsulation in cages is determined by the shape and size of the counteranions, the host-guest redox dependence of the cage can also be considered as an anion-controlled property.

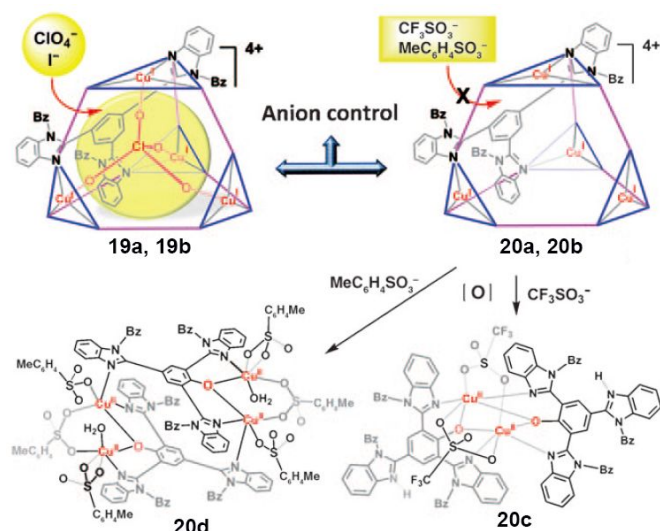


Fig. 24 Guest dependent redox of Su cage **19** and **20**. Reproduced in part with permission from WILEY-VCH Verlag GmbH & Co. KGaA, Weinheim from reference 77.

To make use of such redox-regulable cages as practical catalysts, the authors found an appropriate guest anion (NO_3^-) that can combine the stability of cage **19** and the activity of cage **20**.^[78] The catalytic conversion of tetralin within these cages indicated that all four cage complexes can promote catalytic oxidation (Figure 25), however, the NO_3^- -guested cage **20e** exhibited superior activity to other cages under the same conditions. This is due to the small, planar NO_3^- counteranions, which leave part of the Cu^+ site active for out-cage intermolecular reaction, thus providing a favorable supramolecular model that balances solution stability with robust reactivity for homogeneous catalysis. Similar results were observed for oxidations of indole and tantalum.

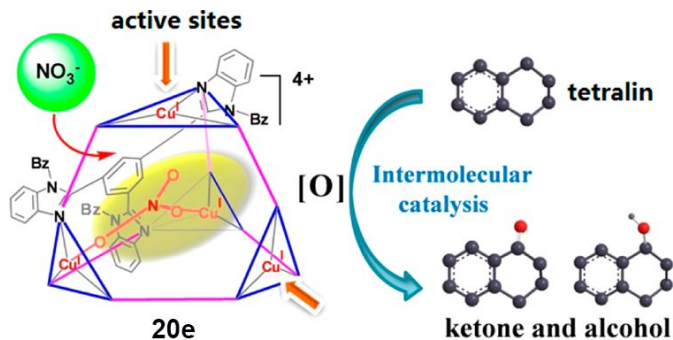


Fig. 25 Tetralin oxidation catalyzed by Su cage **20e**. Reproduced in part with permission from American Chemical Society from reference 78.

3.3 Encapsulated Catalysts within the Cage

Because of their intrinsic porosity, coordination cages can encapsulate a variety of catalysts within their cavities. Catalysts can be introduced into the cavity by either covalent bonding or non-covalent interactions. Although the catalytic reactions take place around the encapsulated catalyst and not at the cage itself, the cavity serves as a flask or vessel, resulting in greater control over guest selectivity and product regio- and stereoselectivity. Furthermore, the cage can efficiently separate catalyst molecules spatially, preventing self-

quenching and deactivation. Since a single cage can encapsulate more than one catalyst, the local concentration of the encapsulated catalyst can be dramatically enhanced. In addition, the morphology of the encapsulated catalyst can be tuned by the cage framework, yielding a highly active species of the catalyst. This section will discuss cage-encapsulated catalysts according to their roles and functions.

3.3.1 Substrate size and shape selectivity

From 2004, the Raymond group devoted substantial effort to encapsulating noble metal complexes in coordination cages to use them as catalysts. They applied their traditional anionic $[\text{M}_4\text{L}_6]^{12-}$ cage **3** to encapsulate a half-sandwich complex $[\text{Cp}^*(\text{PMe}_3)\text{Ir}(\text{Me})\text{OTf}]$.^[79] It was found that mono-cationic iridium intermediate $[\text{Cp}^*(\text{PMe}_3)\text{Ir}(\text{Me})]^+$ was trapped within the cavity of cage **3**, to form a complex **Ir@3** (Figure 26a). Interestingly, the encapsulated Ir complex retains its reactivity towards aldehydes. At 75 °C, the ethene ligand of the encapsulated Ir complex can dissociate, which facilitates the Ir center to activate the C-H bond of an aldehyde. This forms an iridium acyl intermediate, $[\text{Cp}^*(\text{PMe}_3)\text{Ir}(\text{Me})(\text{CO})]^+$, stoichiometrically within the cavity. Furthermore, a variety of aldehyde substrates were examined to investigate the reaction specificity (Figure 26b). It was found that the reactions proceed only when the aldehyde contain relatively small substituted groups (methyl, ethyl, and propyl). Since the cage is chiral, the asymmetric host framework induces the product formation with a diastereomeric ratio (d.r.) ranging from 55:45 to 70:30. This is the first example of C-H activation by an encapsulated catalyst within the cavity of supramolecular assembly. Although this reaction is not catalytic, the results highlighted the potential of encapsulated catalysts and paved the way for further expanding this concept to supramolecular catalysis. In 2006, Raymond's group studied the scope and mechanism of the C-H bond activation by the iridium species within the cavity of the supramolecular cage. They found that the reaction was furnished by a stepwise ion pair co-encapsulation, followed by guest dissociation.^[80]

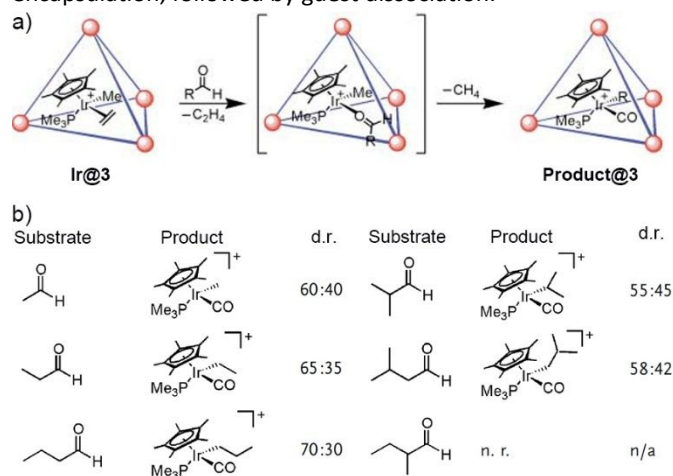


Fig. 26 C-H activation catalyzed by Raymond cage **Ir@3**. Reproduced in part with permission from WILEY-VCH Verlag GmbH & Co. KGaA, Weinheim from reference 79. Reproduced in part with permission from American Chemical Society from reference 80.

In 2007, Raymond and co-workers reported a selective supramolecular encapsulation of bis-phosphine rhodium complexes that display catalytic activity controlled by the size and shape of the host framework **3** (Figure 27a).^[81] They confirmed that cage **3** encapsulated Rh complexes such as $[(\text{PEt}_3)_2\text{Rh}(\text{COD})]^+$ (COD: 1,5-cyclooctadiene) to form a catalyst composite **Rh@3**. When exposed to 1 atm. H_2 , this Rh complex can be efficiently converted to a reactive species, $[(\text{PEt}_3)_2\text{Rh}(\text{OD}_2)_2]^+$, while encapsulated. This reactive Rh species acts as C-H bond activator and catalyzes isomerization of allylic alcohols and ethers. The authors conducted a series of allylic alcohol isomerizations using either the encapsulated Rh catalyst or the free catalyst. Interestingly, they found that 10 mol% of the host-guest catalyst effectively facilitates the and exhibits highly specific substrate size and shape selectivity (Figure 27b). The results clearly demonstrate that a supramolecular microenvironment is capable of controlling catalytic reactivity at metal centers, mimicking the behavior of natural enzymes.

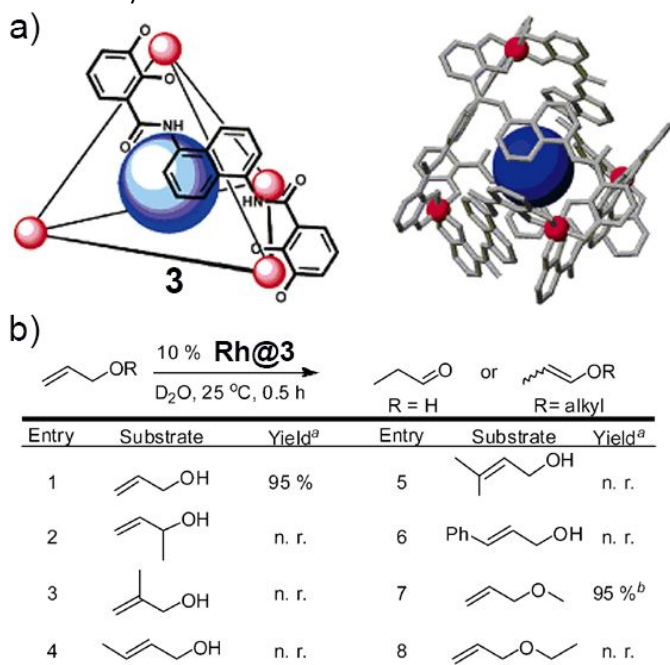


Fig. 27 C-H activation catalyzed by Raymond cage **Rh@3**. Reproduced in part with permission from American Chemical Society from reference 81.

In 2011, the same group reported the encapsulation of a gold-phosphine complex by cage **3** using gallium ions as the metal knots.^[82] One equivalent of Me_3PAu^+ or Et_3PAu^+ cation was encapsulated within the cavity of the cage, as shown by ^1H NMR spectroscopy. Because the hydroalkoxylation of allenes catalyzed by Au complexes has been well documented, they applied the host-guest catalyst for this system to verify its activity (Figure 28). In bulk solution, the hydroalkoxylation of the allenyl alcohol substrate in the presence of Me_3PAuCl catalyst was only achieved an 11% yield after 18 h. In contrast, the catalyst-cage composite, **Au@3**, improved the yield to 48% for the same substrate and could be performed in water. If a

“blocking” reagent, PEt_4^+ pre-occupied the cavity of the cage, only 11% conversion to the cyclized product was observed after 18 h, which strongly indicates that the reaction takes place within the cavity of the cage. The results constitute the first example of acceleration of a gold-catalyzed reaction while encapsulated in a coordination cage.

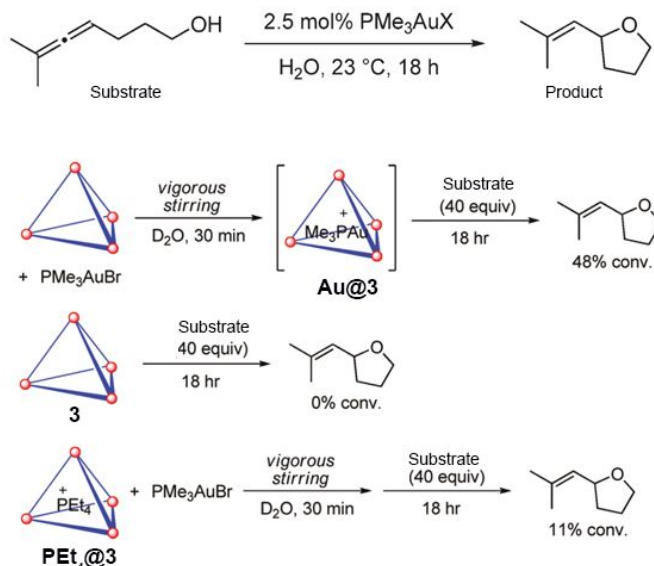


Fig. 28 Allene hydroalkoxylation catalyzed by Raymond cage **Au@3**. Reproduced in part with permission from American Chemical Society from reference 82.

Prior to 2015, the combination of natural enzymes and supramolecular cages for catalyzing organic reactions had never been achieved. In 2015, the Raymond and Toste groups were the first to demonstrate tandem catalysis between gold or ruthenium complexes encapsulated within cage **3** and esterases, lipases or alcohol dehydrogenases.^[83] The reactions studied involved two steps, with the natural enzymes catalyzing one step and the gold/ruthenium species catalyzing the other. When performed in bulk solution, the enzyme often interacts with metal catalyst, deactivating one or both of the catalysts and ceasing the target reaction. However, if the metal catalyst is encapsulated in a coordination cage, the cage can prevent interactions between the enzyme and the metal catalyst, thus eliminating any potential denaturing of the enzymic activity. They obtained host-guest catalysts, **Au@3** and **Ru@3**, by encapsulating Et_3PAu^+ and $(\text{Me}_3\text{P})\text{CpRu}(\text{NCMe})_2^+$ in the cavity of cage **3**. In the first demonstration of this concept, they performed tandem enzyme-mediated acetate hydrolysis followed by **Au@3** or **Ru@3** mediated hydroalkoxylation or olefin isomerization (Figure 29a). Remarkably, **Au@3** exhibits improved conversion over free Au catalyst in all cases. (Figure 29a).

As a second model reaction, the authors performed the **Ru@3**-mediated olefin isomerization of allyl alcohol to give propanal followed by reduction to propanol via ADH (Figure 29b). Neither the enzymes nor the ruthenium catalyst alone can catalyze both reactions in the sequence. This research

demonstrated that encapsulation of the ruthenium catalyst by a coordination cage can prevent adverse interactions between the catalyst and the enzyme, thus making the tandem reaction more efficient. The development of novel catalyst-cage systems for tandem catalysis was able to integrate chemical and biological process.

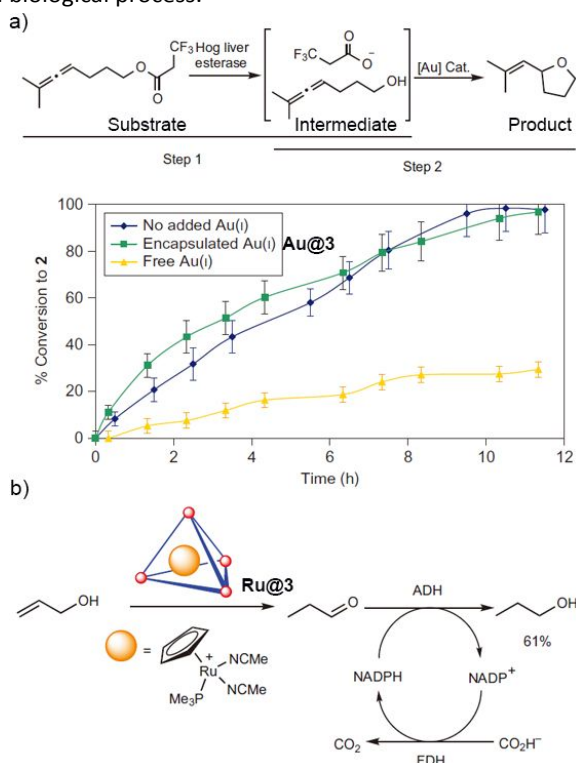


Fig. 29 Tandem reactions catalyzed by Raymond cages Au@3 or Ru@3 coupled with enzymes. Reproduced in part with permission from Springer Nature from reference 83.

The same group reported high valent gold and platinum catalysts encapsulated within coordination cages **3a** and **4a** for alkyl-alkyl reductive elimination (Figure 30a).^[84] As little as 10 mol% of the cage is capable of catalyzing the ethane elimination from a Au(III) iodide complex, giving a 4000-fold initial rate acceleration. Increasing the size of the substituted groups on the Au(III) iodide complex significantly diminished the reaction rate, indicating size exclusion from the cage cavity is the rate determining step. When replacing the gold catalyst with a platinum dialkyl complex with X-type ligands, the elimination rate of ethane was only increased by a factor of 2300. Kinetic experiments revealed the reaction mechanism is Michaelis-Menten-type, involving a halide dissociation, an encapsulation equilibrium and an irreversible reductive elimination (Figure 30b). The key role of the cage is the stabilization of intermediate. In these reactions, the catalyst-cage composite is capable of overcoming kinetically unfavorable energy barriers, thus enhancing the reactivity. This type of model reaction is a dual catalytic cross-coupling reaction in which both the supramolecular microenvironment (cavity) and the transition metal center (catalyst) are necessary and work synergistically, in order to obtain high turnover.

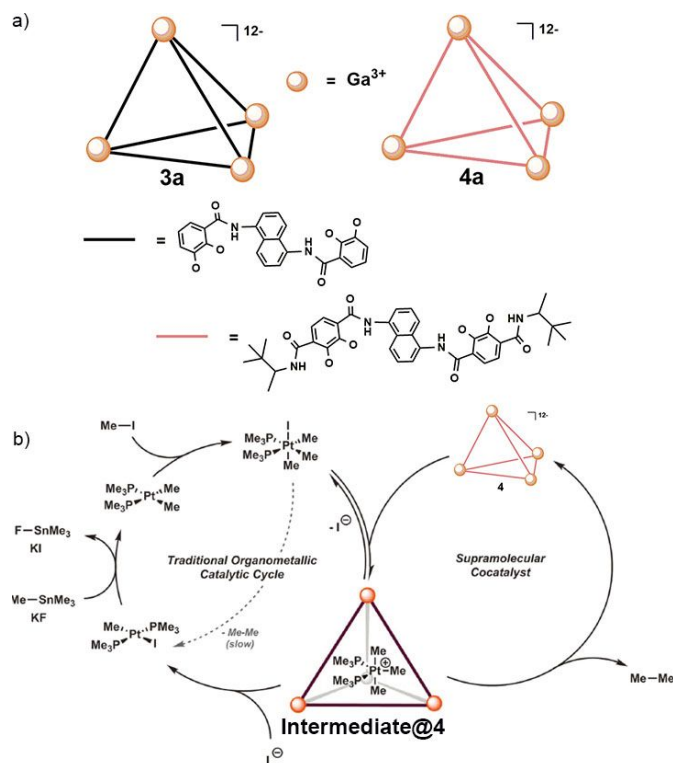


Fig. 30 Alkyl-alkyl reductive elimination catalyzed by Raymond cage **3** and **4**.

3.3.2 Preventing De-activation of Catalysts

Fujita and coworkers designed a sophisticated two-cage system that could catalyze allylic oxidation followed by Diels-Alder cycloaddition. Without the cage capsule, the Diels-Alder (DA) catalyst, MacMillan's catalyst, would be oxidized by the allylic oxidation catalyst, TEMPO.^[85] The researchers managed to incorporate these catalysts into the self-assembled $M_{12}L_{24}$ cages to prevent the deactivation of both catalysts by covalently linking them to the ligand of the cage. Thanks to the unique structure of the $M_{12}L_{24}$ -type cage **21**, which is constructed with 12 Pd(II) ions and 24 bent ditopic ligands, the sphere-like cages possess a robust framework with a large cavity to house catalytic centers and many apertures for the permeation of small substrates. The ligand can be modified to have catalytic moieties, with the catalytic sites of the functionalized ligand pointing towards the internal cavity when the cage is formed. The authors obtained two catalyst-cage composites, **TEMPO@21**, and **DA@21**, with encapsulated TEMPO and MacMillan's catalyst respectively (Figure 31). In the cascade reaction, the substrate was first oxidized to the α,β -unsaturated aldehyde by **TEMPO@21**. Through intramolecular DA cyclization, the α,β -unsaturated aldehyde was then converted to the bicyclic compound by **DA@21** (Figure 31). The obtained product has four adjacent stereogenic centers and is synthesized with high enantio- and diastereoselectivity. As confirmed by the control experiments, neither of the two cages alone can complete the cascade reaction. Only the combination of the two cages' catalysts would allow the desired reaction to proceed. This study provides a basis for the easy design of one-pot chemical

cascade reactions with improved compatibility of the different catalytic requirements.

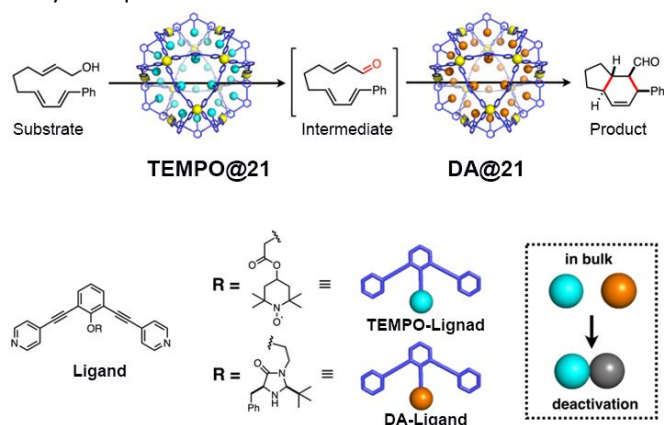


Fig. 31 Tandem reaction catalyzed by Fujita cage TEMPO@21 and DA@21. Reproduced in part with permission from American Chemical Society from reference 85.

3.3.3 Increasing catalyst local concentration

Gold catalysts have gained increased attention in catalysis as they have been demonstrated to facilitate a wide range of reactions, such as cyclization, hydration and oxidation reactions. One of the biggest issues for homogeneous catalytic reactions is that the concentration of the catalyst cannot easily be increased. Some organometallic catalysts, such as gold(I) chloride, have poor solubility in organic solvents, thus reducing the maximum possible catalyst loading. However, some organometallic catalysts can be both installed on the cage ligand and condensed in the cavity once the cage is formed to significantly increase the local concentration of the designated catalyst. In 2014, Reek and co-workers successfully functionalized Fujita's $M_{12}L_{24}$ -type cage **21** with a series of transition metal complexes and, in turn, studied their catalytic activities. [86-88] The first example is a gold functionalized catalyst, **Au@21**. They prepared a gold-functionalized ditopic ligand (**Q**) and synthesized the cage by reacting the ligand with a palladium salt (Figure 32a). Since there're 24 ligands in the cage components, 1 mol of the cage contains 24 mol of the gold catalyst at the most. By varying the ratio of organic ligands (**Q** and **R**) during the synthesis of the cage, the local concentration of gold in the cages could be modulated from 0.05 to 1.07 M. Compared to the low concentration (10^{-6} M) of the gold catalyst in bulk solution, the concentration of the gold catalyst within cage **21** can be significantly increased to 1.07 M, which is 10,000-fold increase (Figure 32b). In addition, they can finely tune the concentration of the gold catalyst within the cage, by tuning the ratio between ligand **Q** and unfunctionalized ligand **R**. At increased catalyst local concentration, catalytic hydroalkoxylation of the allenol by the catalyst-cage composite **Au@21** has 90% yield and 1.86 of TON (Figure 32c). They also found that [4+2] cycloaddition of a variety of diene substrates can be promoted by the same catalyst. [87] The overall conversion of the substrate is effectively quantitative and has tunable selectivity. These works proved that a post-synthetically modified coordination

cage is an effective approach to introducing active site and promotes reactions. By varying the catalyst, coordination cages can serve as a multifunctional catalytic platform for catalysis to obtain high yield, TON and desired selectivity.

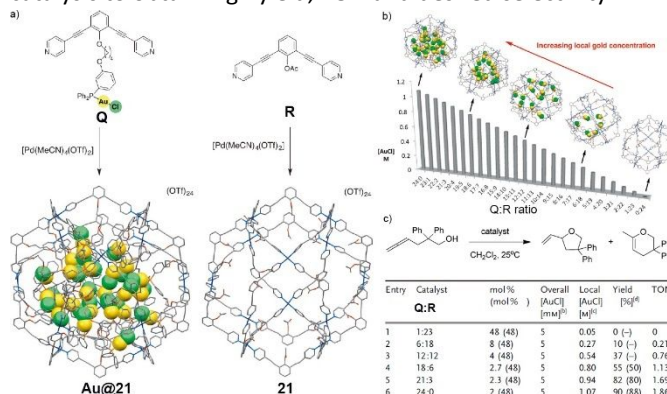


Fig. 32 Hydroalkoxylation catalyzed by Reek cage Au@21. Reproduced in part with permission from WILEY-VCH Verlag GmbH & Co. KGaA, Weinheim from reference 86-88.

The same group made progress in water oxidation catalysis using a similar strategy in 2018. [88] They focused on a ruthenium complex, Ru(bda)Het₂ (bda=2,2'-bipyridine-6,6'-dicarboxylate; Het= aromatic N-heterocycles), which shows excellent activity in oxygen bond formation. They first synthesized cage **21** with guanidinium-functionalized ligands to which sulfonate containing catalysts can be strongly bound through hydrogen bonds. The ruthenium complexes were encapsulated within the cage to form catalyst **Ru@21**, increasing the concentration of the Ru species from 10^{-5} M to 0.54 M. Moreover, **Ru@21** shows a four-fold increase in catalytic current compared to the free catalyst in solution, with a maximum rate of 125 s^{-1} , more than 130 times higher than that observed for the nonencapsulated system (0.93 s^{-1}). Increasing the local concentration of the catalyst through a supramolecular strategy is an important new method to study electrocatalysis.

3.3.4 Tuning Morphology and Size of Encapsulated NPs Catalyst

Because of their tunable cavity size and controllable cavity environment, coordination cages can also act as nanocontainers to trap nanoparticles. The encapsulated nanoparticles are efficiently prevented from aggregating and show mono-distributed particle size, unusual morphology, and higher catalytic activity.

Liao and co-workers synthesized a new trigonal prismatic coordination cage, cage **22**, with calix[4]arene and a 2,5-thiophenedicarboxylic acid (TDC) ligand (Figure 33a). [89] The TDC ligand was embedded in the cage framework and pointed toward the cavity, allowing the formation of strong interactions with encapsulated platinum nanoclusters (Pt). Because of the suitable cavity size and covalent bond between the sulfur and Pt atoms, the cage efficiently encapsulates Pt (ca. 18 Pt atoms), limits the size of the nanoclusters, and binds the nanoclusters tightly. Since Pt nanoclusters are the most

efficient catalyst for hydrogen evolution reactions (HER), the catalyst composite **Pt@22** was then used for a model HER reaction. **Pt@22** exhibited much higher electrocatalytic activity for HER when compared to commercial Pt/C (Figure 33b). This example clearly demonstrates that the size of the nanoparticles can be tuned by the cavity of the coordination cage. Furthermore, the formation of strong interactions between the encapsulated nanoclusters and the cage framework offers an opportunity to obtain the high-performance catalytic composite.

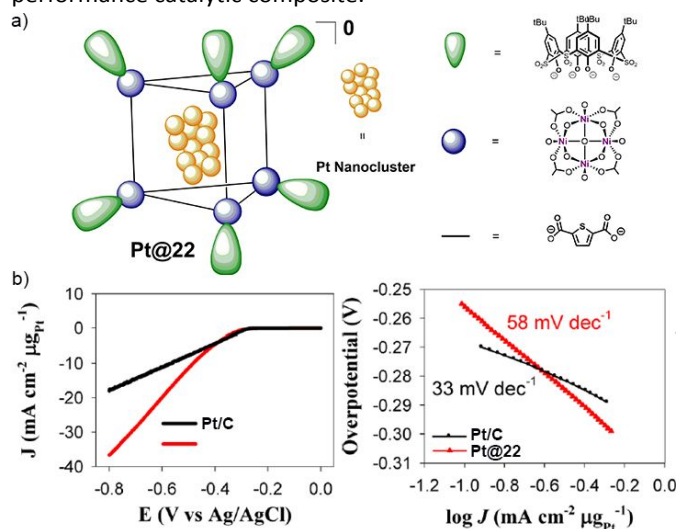


Fig. 33 HER reaction catalyzed by Liao cage **Pt@22**. Reproduced in part with permission from American Chemical Society from reference 89.

In 2018, Zhou and co-workers also reported a newly designed octahedral coordination cage, cage **23a**, with 30 negative charges (Figure 34).^[90] The anionic nature of the cage endows the cage with the ability to efficiently trap the nanoparticle precursors, the metal salts. Additionally, once the nanoparticles are encapsulated by the charged cage shell, the charge repulsions between individual caged nanoparticles will prevent aggregation. Thus, they applied this cage to encapsulate Ru nanoparticles (Ru). They found that the encapsulated Ru nanoparticles show an unusual *face-centered-cubic (fcc)* single crystal phase, with ultra-small size (2.5 nm) and a highly dispersed form. More importantly, the cage-nanoparticle composite, **Ru@23a**, was proved to be the most efficient catalyst for the methanolysis of ammonia borane, with a record-high turnover frequency (TOF, 304.4 min⁻¹). This result provides insights into the engineering of catalytic properties through a host-guest method.

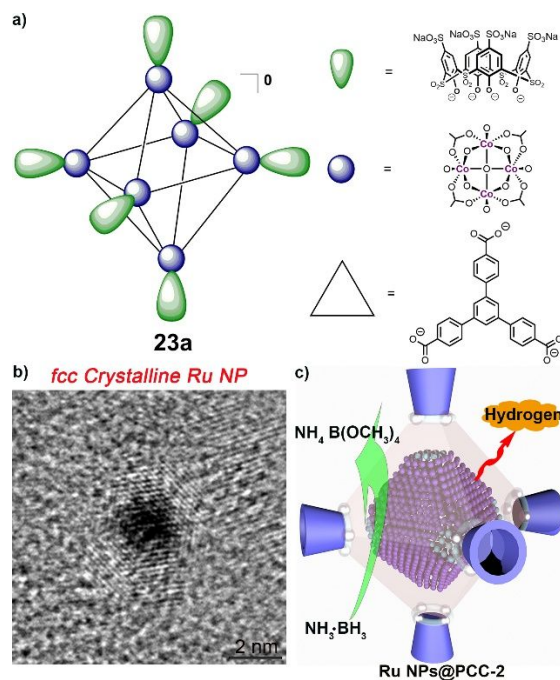


Fig. 34 Methanolysis reaction catalyzed by Zhou cage **Ru@23a**.

Compared to noble metal nanoparticles, first-row transition-metal nanoclusters are notorious for low reactivity in the dehydrogenation of ammonia borane. The intrinsic reason for this is the poor molecular orbital overlap between the nanoclusters and ammonia borane. Additionally, first-row transition-metal nanoclusters are easily oxidized under ambient conditions. Zhou's group applied cage **23a** to encapsulate first-row transition-metal nanoclusters and systematically investigated the charge effect of the cage on the formation of the nanoclusters using **23a** and its analog, **23b**, which has only 6 negative charges (Figure 35).^[91] When they applied both the two cages to encapsulate cobalt nanoclusters (Co), only the highly negatively charged **23a** could encapsulate Co and form a homogeneous catalyst composite, **Co@23a**. In contrast, **23b** gives precipitation of the cobalt nanoparticles, indicating phase separation of the nanoclusters and the cage. High-resolution TEM (HR-TEM) analysis shows that **Co@23a** has a uniform particle size with a 2.5 nm diameter. However, the **Co/23b** mixture has a much larger particle size (> 100 nm) than that of **Co@23a** and shows a highly aggregated form. When applying the two cage-catalyst composites in the hydrolysis of ammonia borane, they showed divergent performance. Again, **Co@23a** exhibits record-high TOF in the dehydrogenation reaction, while **Co/23b** shows no significant impact on the reactivity. This research demonstrates that the electronic property of the host affects the formation of the encapsulated nanoparticles.

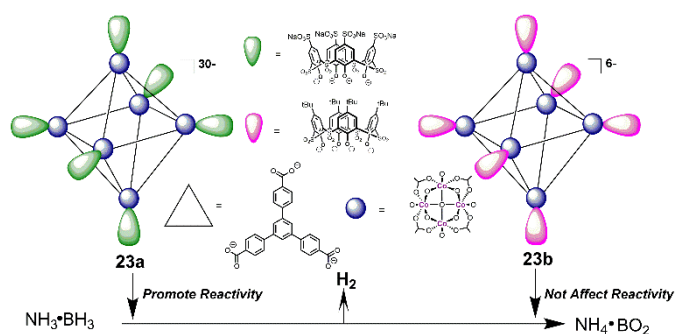


Fig. 35 Hydrolysis reaction catalyzed by Zhou cage Co@23.

3.3.5 Putting catalyst and substrate close proximity

Artificial catalysts sometimes show low reactivity because of the low binding affinity to the substrates, particularly when the two have the same charge. In the contrary, natural enzymes do not have this issue. The enzyme binds the reactants within its pockets, reduces the distance with the substrates and increases the reaction occurrence. Inspired by the enzymatic behavior, coordination cages can be engineered to co-encapsulate metal catalyst with organic substrate, in order to improve the catalytic reactivity. Zhou *et al.* prepared an anionic coordination cage **23a** and applied it in encapsulating cationic [Ru(bpy)₃]²⁺Cl₂ (bpy = bipyridine) catalyst (Ru) and to form a host-guest complex **Ru@23a** (Figure 36).^[92] Then, they used the Ru catalyst and the **Ru@23a** in the photodegradation of organic dye, methylene blue (MB). In homogenous state, the Ru catalyst shows moderate dye degradation activity, because of the charge repulsion between the two cationic species. Only 19.8% of MB was degraded by Ru catalyst after 240 min under visible light irradiation. Under the same condition, **Ru@23a** dramatically improved the degradation of MB to 94.9%. When they investigated the reaction kinetics of the photodegradation profile, **Ru@23a** shows an about 5 times larger rate constant ($2.09 \times 10^{-2} \text{ min}^{-1}$), than that for the homogeneous Ru catalyst ($0.06 \times 10^{-2} \text{ min}^{-1}$). This catalyst-cage system is one of best efficient catalyst composites even when comparing to other Ru-doped or Ru-immobilized MOF systems. Further study on the reaction mechanism suggested that the reaction adopts an oxidative pathway which is similar to the previously reported TiO₂ catalyzed one. The key for the efficiency promotion in this photocatalytic reaction is that the highly charged anionic cage puts the cationic catalyst and cationic into close reaction proximity. The further engineering of the cage in charge and cavity is capable of explore novel reactions and improving reactions efficiencies.

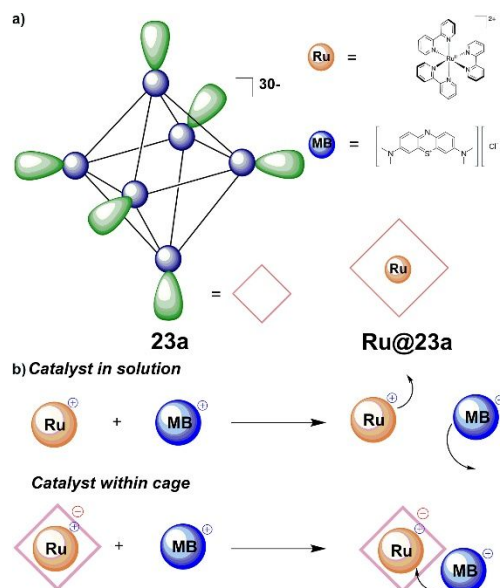


Fig. 36 Dye degradation catalyzed by Zhou cage Ru@23a.

Summary and Outlook

Since the pioneers of this field first defined supramolecular hosts 40 years ago, the development of coordination cages has greatly advanced to achieve enzyme-mimic catalysis. The last 10 years have witnessed the rapid growth of supramolecular catalysis, taking advantage of the geometric diversity and functionality tunability of the self-assembled hosts.^[31-92] A variety of catalytic reactions within the cavity of supramolecular hosts have been carefully examined to elucidate the reaction mechanisms. As a result, specific catalytic reactions can be designed, anticipated, and performed within the cavity of supramolecular hosts, such as coordination cages. More importantly, the reactivity, regioselectivity and enantioselectivity can be manipulated by engineering the structural and electronic properties of the cage frameworks. These features make coordination cages an innovative and promising platform for catalysis research.

Although supramolecular catalysis, particularly coordination cage catalysis, has been investigated for less than 20 years, this emerging field has seen tremendous progress and will be further pursued because of the broad interest in “enzyme mimics”. As model compounds of synthetic hosts that mimic the structure and function of a natural enzyme, coordination cages have intrinsic advantages. (1) As a discrete self-assembled system, coordination cages have a similar size to many enzymes. In the early days of coordination cage chemistry, the structures of the cages only had a handful of components and very small diameters (< 0.2 nm). Recently, however, giant cage compounds can be built with up to 144 components with a 10 nm overall diameter, comparable to natural proteins. (2) The guest-binding cavities of coordination cages are comparable to the substrate-binding sites of enzymes. Although it is not possible to replicate the complicated protein structure with a supramolecular assembly,

coordination cages have a substrate-binding cavity, which is a crucial element of an enzyme. The cavity of a coordination cage can perform substrate encapsulation, molecular transformation, intermediate capturing, and product release, which facilitate the catalytic cycle. (3) The crystalline state of coordination cages makes it possible to control the structure and functionality of the cage at an atomic level. Despite many species having been applied as catalysts, few of them are used in a crystalline state. Because of the ordered alignment and reversible formation of coordination bonds, the structures of coordination cages can be solved by taking advantage of modern X-ray crystallographic technology. Therefore, it is possible to study the structure-property relationship in detail. (4) The electronic properties of coordination cages can be facily tuned. While proteins usually bear a negative charge, the charge of a coordination cage can be manipulated to be positive, negative or neutral by choosing a suitable coordination site or by directly introducing cationic or anionic cage components. The electronic properties of the host frameworks serve as the driving force for binding substrate molecules.

In addition, coordination cages also have some advantages when compared to other porous networked materials, such as metal-organic frameworks (MOFs) and covalent-organic frameworks (COFs).^[96-100] First of all, the homogeneous nature of coordination cages allows the investigation of catalytic properties in solvated media. While the permanent porosity of MOFs and COFs renders them as promising heterogeneous catalysts that take advantage of the confined effect, they behave as solid phases that suffer from diffusion problems in mass transportation. This problem could potentially be solved by introducing hierarchical pores into those solid porous catalysts, however at present, homogeneous catalysts, enzymes, and coordination cages usually exhibit much higher catalytic activity. Secondly, it is much easier to monitor catalytic processes mediated by coordination cages than those by solid catalysts. Many spectroscopic techniques, such as NMR, UV-Vis, and fluorescence spectroscopy, have been widely applied to monitor reactions catalyzed by coordination cages. In some cases, it is possible to directly observe structure/property transitions of the encapsulated compound and the interactions between the cage and the substrate/product.

This review has emphasized a state-of-the-art applications of coordination cages to catalytic reactions. Through the combination of embedded catalysts, encapsulated catalysts, and cavity-promoted reactions discussed herein, it is becoming increasingly plausible to rationally design coordination cage-based catalytic systems, even those involving complicated multi-step catalytic reactions beyond what can currently be achieved. These recent advances represent the beginnings of a powerful complement to the tandem/cascade processes employed in conventional organometallic catalysis and other porous solid-based catalysis. The continued exploration of the fundamental mechanisms of coordination cage catalysis will

ultimately lead to advances in reactivity modulation, industrial processes, chemical sensing systems, energy storage, novel energy sources, and drug carriers. Coordination cages will provide good cost-performance value and improve the sustainability of these processes.^[101-113]

Overall, the development of coordination cages for catalysis has emerged as a hot topic in supramolecular chemistry. With well-studied examples and approaches, we envision that more sophisticated and multifunctional coordination cages will be designed and fabricated, and these cages may exhibit reactivity, selectivity, and specificity to rival that of natural enzymes.

Acknowledgments

The authors of this review were each supported in part by Robert A. Welch Foundation through a Welch Endowed Chair to H.J.Z. (A-0030), the NPRP award NPRP9-377-1-080 from the Qatar National Research Fund, and by the U.S. Department of Energy, Office of Science, Office of Basic Energy Sciences, under Award Number DE-SC0017864. We also want to thank the National Natural Science Foundation of China (No. 21401037).

Author Contributions

Original idea was conceived by H.-C.Z and Y.F.; manuscript was drafted by Y.F., J.A.P., and E.L.; figures were prepared by Y.F. and Q.W.; citations were prepared by Q.W. and Z.X.; table was prepared by A.K. and X.Y.; manuscript was revised by C.Z., L.Z., and F.H. All authors have given approval to the manuscript.

References

- [1] A. Stank, D. B. Kokh, J. C. Fuller and R. C. Wade, *Acc. Chem. Res.*, 2016, **49**, 809–815.
- [2] M. Gao and J. Skolnick, *PLoS Comput. Biol.*, 2013, **9**, e1003302.
- [3] J. Dundas, L. Adamian and J. Liang, *J. Mol. Biol.*, 2011, **406**, 713–729.
- [4] D. J. Cram, *Nature*, 1992, **356**, 29–36.
- [5] C. O. Mellet, J. M. G. Fernández and J. M. Benito, *Chem. Soc. Rev.*, 2011, **40**, 1586–1608.
- [6] C. J. Pedersen, *J. Am. Chem. Soc.*, 1967, **89**, 2495–2496.
- [7] D. J. Cram, *Science*, 1983, **219**, 1177–1183.
- [8] J. M. Lehn, *Angew. Chem. Int. Ed.*, 2015, **54**, 3276–3289.
- [9] G. Crini, *Chem. Rev.*, 2014, **114**, 10940–10975.
- [10] V. Böhmer, *Angew. Chem. Int. Ed. Engl.*, 1995, **34**, 713–745.
- [11] A. F. Danil de Namor, R. M. Cleverley and M. L. Zapata-Ormachea, *Chem. Rev.*, 1998, **98**, 2495–2526.

- [12] H. J. Kim, M. H. Lee, L. Mutihac, J. Vicens and J. S. Kim, *Chem. Soc. Rev.*, 2012, **41**, 1173–1190.
- [13] T. S. Koblenz, J. Wassenaar and J. N. H. Reek, *Chem. Soc. Rev.*, 2008, **37**, 247–262.
- [14] A. Galana and P. Ballester, *Chem. Soc. Rev.*, 2016, **45**, 1720–1737.
- [15] M. Raynal, P. Ballester, A. Vidal-Ferran and P. W. N. M. van Leeuwen, *Chem. Soc. Rev.*, 2014, **43**, 1660–1733.
- [16] T. R. Cook, Y.-R. Zheng and P. J. Stang, *Chem. Rev.*, 2013, **113**, 734–777
- [17] M. Liu, W. Liao, C. Hu, S. Du and H. Zhang, *Angew. Chem. Int. Ed.*, 2012, **51**, 1585–1588.
- [18] F.-R. Dai and Z. Wang, *J. Am. Chem. Soc.*, 2012, **134**, 8002–8005.
- [19] S. Durot, J. Taesch and V. Heitz, *Chem. Rev.*, 2014, **114**, 8542–8578;
- [20] D. W. Zhang, A. Martinez and J. P. Dutasta, *Chem. Rev.*, 2017, **117**, 4900–4942.
- [21] M. J. Wiester, P. A. Ulmann and C. A. Mirkin, *Angew. Chem. Int. Ed.*, 2011, **50**, 114–137.
- [22] C. J. Brown, F. D. Toste, R. G. Bergman and K. N. Raymond, *Chem. Rev.*, 2015, **115**, 3012–3035.
- [23] M. Yoshizawa, J. K. Klosterman and M. Fujita, *Angew. Chem. Int. Ed.*, 2009, **48**, 3418–3438.
- [24] T. R. Cook and P. J. Stang, *Chem. Rev.*, 2015, **115**, 7001–7045.
- [25] W. Wang, Y. X. Wang and H. B. Yang, *Chem. Soc. Rev.*, 2016, **45**, 2656–2693.
- [26] D. A. Roberts, B. S. Pilgrim and J. R. Nitschke, *Chem. Soc. Rev.*, 2018, **47**, 626–644.
- [27] W. M. Bloch and G. H. Clever, *Chem. Commun.*, 2017, **53**, 8506–8516.
- [28] Y. F. Han, W. G. Jia, W. B. Yu and G. X. Jin, *Chem. Soc. Rev.*, 2009, **38**, 3419–3434.
- [29] A. M. Castilla, W. J. Ramsay and J. R. Nitschke, *Acc. Chem. Res.*, 2014, **47**, 2063–2073.
- [30] C. Tan, D. Chu, X. Tang, Y. Liu, W. Xuan and Y. Cui, *Chem. Eur. J.*, 2019, **25**, 662–672.
- [31] B. Olenyuk, J. A. Whiteford, A. Fechtenkötter and P. J. Stang, *Nature*, 1999, **398**, 794–796.
- [32] T. Kusakawa, T. Nakai, T. Okano and M. Fujita, *Chem. Lett.*, 2003, **32**, 284–285.
- [33] M. Yoshizawa, M. Tamura and M. Fujita, *Science*, 2006, **312**, 251–254.
- [34] T. Murase, S. Horiuchi, and M. Fujita, *J. Am. Chem. Soc.*, 2010, **132**, 2866–2867.
- [35] Y. Fang, T. Murase, S. Sato and M. Fujita, *J. Am. Chem. Soc.*, 2013, **135**, 613–615.
- [36] Y. Fang, T. Murase and M. Fujita, *Chem. Lett.*, 2015, **44**, 1095–1097.
- [37] D. Fiedler, D. H. Leung, R. G. Bergman and K. N. Raymond, *J. Am. Chem. Soc.*, 2004, **126**, 3674–3675.
- [38] D. H. Leung, D. Fiedler, R. G. Bergman and K. N. Raymond, *Angew. Chem. Int. Ed.*, 2004, **43**, 963–966.
- [39] D. Fiedler, R. G. Bergman and K. N. Raymond, *Angew. Chem. Int. Ed.*, 2004, **43**, 6748–6751.
- [40] D. Fiedler, H. van Halbeek, R. G. Bergman and K. N. Raymond, *J. Am. Chem. Soc.*, 2006, **128**, 10240–10252.
- [41] C. J. Hastings, D. Fiedler, R. G. Bergman and K. N. Raymond, *J. Am. Chem. Soc.*, 2008, **130**, 10977–10983.
- [42] C. J. Brown, R. G. Bergman and K. N. Raymond, *J. Am. Chem. Soc.*, 2009, **131**, 17530–17531.
- [43] Y. Ootani, Y. Akinaga and T. Nakajima, *J. Comput. Chem.*, 2015, **36**, 459–466.
- [44] T. Murase, Y. Nishijima and M. Fujita, *J. Am. Chem. Soc.*, 2012, **134**, 162–164.
- [45] P. H. Campbell, N. W. K. Chiu, K. Deugau, I. J. Miller and T. S. Sorensen, *J. Am. Chem. Soc.*, 1969, **91**, 6404–6410.
- [46] C. J. Hastings, M. D. Pluth, R. G. Bergman and K. N. Raymond, *J. Am. Chem. Soc.*, 2010, **132**, 6938–6940.
- [47] C. J. Hastings, M. P. Backlund, R. G. Bergman and K. N. Raymond, *Angew. Chem. Int. Ed.*, 2011, **50**, 10570–10573.
- [48] C. J. Hastings, R. G. Bergman and K. N. Raymond, *Chem. Eur. J.*, 2014, **20**, 3966–3973.
- [49] C. M. Hong, M. Morimoto, E. A. Kapustin, N. Alzakhem, R. G. Bergman, K. N. Raymond and F. D. Toste, *J. Am. Chem. Soc.*, 2018, **140**, 6591–6595.
- [50] W. M. Hart-Cooper, K. N. Clary, F. D. Toste, R. G. Bergman and K. N. Raymond, *J. Am. Chem. Soc.*, 2012, **134**, 17873–17876.
- [51] W. M. Hart-Cooper, C. Zhao, R. M. Triano, P. Yaghoubi, H. L. Ozores, K. N. Burford, F. D. Toste, R. G. Bergman and K. N. Raymond, *Chem. Sci.*, 2015, **6**, 1383–1393.
- [52] D. M. Kaphan, F. D. Toste, R. G. Bergman and K. N. Raymond, *J. Am. Chem. Soc.*, 2015, **137**, 9202–9205.
- [53] M. D. Pluth, R. G. Bergman and K. N. Raymond, *Science*, 2007, **316**, 85–88.
- [54] M. D. Pluth, R. G. Bergman and K. N. Raymond, *J. Am. Chem. Soc.*, 2007, **129**, 11459–11467.
- [55] M. D. Pluth, R. G. Bergman and K. N. Raymond, *J. Am. Chem. Soc.*, 2008, **130**, 11423–11429.
- [56] M. L. Price, J. Adams, C. Lagenaur and E. H. Cordes, *J. Org. Chem.*, 1969, **34**, 22–25.
- [57] M. D. Pluth, R. G. Bergman and K. N. Raymond, *Angew. Chem.*, 2007, **119**, 8741–8743.
- [58] M. D. Pluth, R. G. Bergman and K. N. Raymond, *J. Org. Chem.*, 2009, **74**, 58–63.
- [59] J. L. Bolliger, A. M. Belenguer and J. R. Nitschke, *Angew. Chem. Int. Ed.*, 2013, **52**, 7958–7962.
- [60] J. L. Bolliger, *Chimia*, 2014, **68**, 204–207.
- [61] P. Das, A. Kumar, P. Howlader and P. S. Mukherjee, *Chem. Eur. J.*, 2017, **23**, 12565–12574.
- [62] W. Cullen, M. C. Misuraca, C. A. Hunter, N. H. Williams and M. D. Ward, *Nat. Chem.*, 2016, **8**, 231–236.
- [63] W. Cullen, A. J. Metherell, A. B. Wragg, C. G. P. Taylor, N. H. Williams and M. D. Ward, *J. Am. Chem. Soc.*, 2018, **140**, 2821–2828.

- [64] A. G. Salles Jr., S. Zarra, R. M. Turner and J. R. Nitschke, *J. Am. Chem. Soc.*, 2013, **135**, 19143–19146.
- [65] J. J. Jiao, Z. Li, Z. Qiao, X. Li, Y. Liu, J. Dong, J. Jiang and Y. Cui, *Nat. Commun.*, 2018, **9**, 4423.
- [66] F.-R. Dai, Y. Qiao and Z. Wang, *Inorg. Chem. Front.*, 2016, **3**, 243–249.
- [67] F.-R. Dai, L. Zhang, J. Li, W. Lin and Z. Wang, *Angew. Chem. Int. Ed.*, 2016, **55**, 12778–12782.
- [68] G.-J. Chen, C.-Q. Chen, X.-T. Li, H.-C. Ma and Y.-B. Dong, *Chem. Commun.*, 2018, **54**, 11550–11553.
- [69] W. Lu, D. Yuan, A. Yakovenko and H.-C. Zhou, *Chem. Commun.*, 2011, **47**, 4968–4970.
- [70] T. Gadzikwa, R. Bellini, H. L. Dekker and J. N. H. Reek, *J. Am. Chem. Soc.*, 2012, **134**, 2860–2863.
- [71] C. He, J. Wang, L. Zhao, T. Liu, J. Zhang and C. Duan, *Chem. Commun.*, 2013, **49**, 627–629.
- [72] J. Guo, Y.-W. Xu, K. Li, L.-M. Xiao, S. Chen, K. Wu, X.-D. Chen, Y.-Z. Fan, J.-M. Liu and C.-Y. Su, *Angew. Chem. Int. Ed.*, 2017, **56**, 3852–3856.
- [73] J. Jiao, C. Tan, Z. Li, Y. Liu, X. Han and Y. Cui, *J. Am. Chem. Soc.*, 2018, **140**, 2251–2259.
- [74] C. Tan, J. Jiao, Z. Li, Y. Liu and Y. Cui, *Angew. Chem. Int. Ed.*, 2018, **57**, 2085–2090.
- [75] M. Otte, P. F. Kuijpers, O. Troeppner, I. Ivanović-Burmazović, J. H. H. Reek and B. De Bruin, *Chem. Eur. J.*, 2013, **19**, 10170–10178.
- [76] L. R. Holloway, P. M. Bogie, Y. Lyon, C. Ngai, T. F. Miller, R. R. Julian and R. J. Hooley, *J. Am. Chem. Soc.*, 2018, **140**, 8078–8081.
- [77] Q.-T. He, X.-P. Li, Y. Liu, Z.-Q. Yu, W. Wang and C.-Y. Su, *Angew. Chem. Int. Ed.*, 2009, **48**, 6156–6159.
- [78] Q.-T. He, X.-P. Li, L.-F. Chen, L. Zhang, W. Wang and C.-Y. Su, *ACS Catal.*, 2013, **3**, 1–9.
- [79] D. H. Leung, D. Fiedler, R. G. Bergman and K. N. Raymond, *Angew. Chem. Int. Ed.*, 2004, **43**, 963–965.
- [80] D. H. Leung, R. G. Bergman and K. N. Raymond, *J. Am. Chem. Soc.*, 2006, **128**, 9781–9797.
- [81] D. H. Leung, R. G. Bergman and K. N. Raymond, *J. Am. Chem. Soc.*, 2007, **129**, 2746–2747.
- [82] Z. J. Wang, C. J. Brown, R. G. Bergman, K. N. Raymond and F. D. Toste, *J. Am. Chem. Soc.*, 2011, **133**, 7358–7360.
- [83] Z. J. Wang, K. N. Clary, R. G. Bergman, K. N. Raymond and F. D. Toste, *Nat. Chem.*, 2015, **5**, 100–103.
- [84] D. M. Kaphan, M. D. Levin, R. G. Bergman, K. N. Raymond and F. D. Toste, *Science*, 2015, **350**, 1235–1238.
- [85] Y. Ueda, H. Ito, D. Fujita and M. Fujita, *J. Am. Chem. Soc.*, 2017, **139**, 6090–6093.
- [86] R. Gramage-Doria, J. Hessels, S. H. A. M. Leenders, O. Tröppner, M. Dürr, I. Ivanović-Burmazović and J. N. H. Reek, *Chem. Eur. J.*, 2014, **53**, 13380–13384.
- [87] S. H. A. M. Leenders, M. Dürr and J. N. H. Reek, *Adv. Synth. Catal.*, 2016, **358**, 1509–1518.
- [88] F. Yu, D. Poole III, S. Mathew, N. Yan, J. Hessels, N. Orth, I. Ivanović-Burmazović and J. N. H. Reek, *Angew. Chem. Int. Ed.*, 2018, **57**, 11247–11251.
- [89] S. Wang, X. Gao, X. Hang, X. Zhu, H. Han, W. Liao and W. Chen, *J. Am. Chem. Soc.*, 2016, **138**, 16236–16239.
- [90] Y. Fang, J. Li, T. Togo, F. Jin, Z. Xiao, L. Liu, H. Drake, X. Lian and H.-C. Zhou, *Chem*, 2018, **4** (3), 555–563.
- [91] Y. Fang, Z. Xiao, J. Li, C. Lollar, L. Liu, X. Lian, S. Yuan, S. Banerjee, P. Zhang and H.-C. Zhou, *Angew. Chem. Int. Ed.*, 2018, **57**, 5283–5287.
- [92] Y. Fang, Z. Xiao, A. Kirchon, J. Li, F. Jin, T. Togo, L. Zhang, C. Zhu, and H.-C. Zhou, *Chem. Sci.*, 2019, **10**, 3529–3534.
- [93] Y. Bai, Y. Dou, L.-H. Xie, W. Rutledge, J.-R. Li and H.-C. Zhou, *Chem. Soc. Rev.*, 2016, **45**, 2327–2367.
- [94] G. Liu, Z. Ju, D. Yuan and M. Hong, *Inorg. Chem.*, 2013, **52**, 13815–13817.
- [95] Z. Ju, G. Liu, Y. S. Chen, D. Yuan and B. Chen, *Chem. Eur. J.*, 2017, **23**, 4774–4777.
- [96] M. Bhadra, H. S. Sasmal, A. Basu, S. P. Midya, S. Kandambeth, P. Pachfule, E. Balaraman and R. Banerjee, *ACS Appl. Mater. Interfaces*, 2017, **9**, 13785–13792.
- [97] H. L. Nguyen, F. Gandara, H. Furukawa, T. L. H. Doan, K. E. Cordova and O. M. Yaghi, *J. Am. Chem. Soc.*, 2016, **138**, 4330–4333.
- [98] B. Aguila, Q. Sun, X. L. Wang, E. O. Rourke, A. M. Al-Enizi, A. Nafady and S. Ma, *Angew. Chem. Int. Ed.*, 2018, **57**, 10107–10111.
- [99] Q. Sun, B. Aguila, J. Perman, N. Nguyen and S. Ma, *J. Am. Chem. Soc.*, 2016, **138**, 15790–15796.
- [100] X. Han, Q. Xia, J. Huang, Y. Liu, C. Tan and Y. Cui, *J. Am. Chem. Soc.*, 2017, **139**, 8693–8697.
- [101] Q.-L. Zhu and Q. Xu, *Chem. Soc. Rev.*, 2014, **43**, 5468–5512.
- [102] M. Han, D. M. Engelhard and G. H. Clever, *Chem. Soc. Rev.*, 2014, **43**, 1848–1860.
- [103] H. Amouri, C. Desmarets and J. Moussa, *Chem. Rev.*, 2012, **112**, 2015–2041.
- [104] K. D. Hänni and D. A. Leigh, *Chem. Soc. Rev.*, 2010, **39**, 1240–1251.
- [105] B. Zheng, F. Wang, S. Dong and F. Huang, *Chem. Soc. Rev.*, 2012, **41**, 1621–1636.
- [106] Q. Yang, Q. Xu and H.-L. Jiang, *Chem. Soc. Rev.*, 2017, **46**, 4774–4808.
- [107] D. Shetty, J. K. Khedkar, K. M. Park and K. Kim, *Chem. Soc. Rev.*, 2015, **44**, 8747–8761.
- [108] H. N. Miras, L. Vilà-Nadal and L. Cronin, *Chem. Soc. Rev.*, 2014, **43**, 5679–5699.
- [109] M. D. Ward, C. A. Hunter and N. H. Williams, *Acc. Chem. Rev.*, 2018, **51**, 2073–2082.
- [110] L. Catti, Q. Zhang, and K. Tiefenbacher, *Chem. Eur. J.*, 2016, **22**, 9060–9066.
- [111] S. Zarra, D. M. Wood, D. A. Roberts and J. R. Nitschke, *Chem. Soc. Rev.*, 2015, **44**, 419–432.

ARTICLE

Journal Name

[112] S. H. A. M. Leenders, R. Gramage-Doria, B. de Bruin and J. N. H. Reek, *Chem. Soc. Rev.*, 2015, **44**, 433–448.

[113] D. B. Amabilino, D. K. Smith and J. W. Steed, *Chem. Soc. Rev.*, 2017, **46**, 2404–2420.